Drought and climate change: variability and trends in Germany

Master Thesis

Raphael Menke
Albert-Ludwigs-Universität Freiburg
Prof. Dr. Kerstin Stahl
Prof. Dr. Carsten Dormann

April 2, 2019

Men argue. Nature acts.

Voltaire

Contents

List of Figures

List of Tables

List of Figures in the Appendix

Acknowledgements

I acknowledge Jost Hellwig and Kerstin Stahl for providing helpful feedback. I thank all proof-readers. Ruben for the revision of the statistical calculations. I thank Ferdinand, Laurin, Evan and Raphael for checking my English. I thank David for helping me with *ggplot* legend issues. Last but not least, I thank all the numerous contributors of *stackoverflow.com*.

Zusammenfassung

Da die Folgen von Dürren in Mitteleuropa in der jüngsten Vergangenheit vorherrschen, sind Trends bei den Abflüssen von entscheidender Bedeutung, um Überwachungs- und Frühwarnsysteme (M & EW) einrichten zu können. In dieser Studie wurden 337 naturnahe Kopfeinzugsgebiete in Deutschland auf mögliche Trockenheitstrends hin analysiert. Der Mann-Kendall Trendtest wurde auf die Zeitreihen der Jahre 1970 - 2009 angewendet, um saisonale und Niedrigwasser Veränderungen zu ermitteln. Während die Trends der Niedrigwasserabflüsse im Sommer keine kohärente Trendrichtung für ganz Deutschland aufweisen, unterliegen die saisonalen Abflusstrends erheblichen Veränderungen. Diese Studie bestätigt die Ergebnisse europaweiter Studien zu allgemeineren höheren Abflüssen im Winter und Frühling und geringeren Abflüssen im Sommer für Deutschland. Niederschlags- und hydrologischen Dürren wurden in dieser Studie mit einem zeitlich variierenden Schwellenwert ermittelt. Die Dürretrends werden von den Dürrejahren 1971 und 1976 dominiert und zeigen daher vor allem negative Trends bei der Dauer und Schwere der Dürre auf. Da sich die Abflussregimes in Mitteleuropa unter der globalen Erwärmung möglicherweise ändern können, wurden die ermittelten Abflusstrends mit der vorhergesagten Änderung der „Global Circulation Models“ in Beziehung gesetzt. Um die Prozesse zu verstehen, die die Manifestierung der meteorologischen Variablen im hydrologischen Kreislauf steuern, wurde der Zusammenhang zwischen klimatischen Variablen und dem Abfluss während Dürreereignissen analysiert. Um diese Verknüpfung zu messen, wurde die Korrelation des Standardisierten Niederschlags- und Niederschlags-Evapotranspirationsindex (SPI und SPEI) mit dem Standardisierten Streamflow Index (SSI) berechnet. Die Ergebnisse zeigten, dass trotz zunehmender Evapotranspirationstrends die Dürren in Deutschland immer noch durch ein Niederschlagsdefizit und nicht durch höhere Evapotranspirationsraten verursacht werden.

Stichworte: Hydrologische Dürre, Meteorologische Dürre, SPI, SPEI, SSI, Einzugsgebietseigenschaften, Trockenheitsmerkmale, E-OBS, Trends, Deutschland

Abstract

Trends in streamflow are of vital importance to assess the extend of possible future change as the consequences of droughts are predominant in central Europe in the recent past. This study analysis 337 near-natural head catchments in Germany to detect possible trends in streamflow. The Mann-Kendall test was applied to precipitation, temperature and discharge time series of the years 1970 - 2009. While trends in low flows during summer do not exhibit a coherent trend direction for the whole of Germany the seasonal discharge trends are subject to significant changes. This study confirms the results of cross European studies of a general wetting trend in winter and spring and a general drying trend in summer for Germany. The properties and trends of precipitation and hydrological droughts were determined in this study with a varying threshold approach. Drought trends are dominated by the severe droughts in 1971 and 1976 and therefore mainly depict negative values in drought length and severity. Streamflow regimes in central Europe are possibly subject to change under global warming. Detected streamflow trends are put in relation with the predicted output of Global Circulation Models. To understand the processes controlling the propagation from meteorologic to hydrologic drought the relationship between climatic variables and streamflow during drought events were analysed. To measure this linkage, the correlation of the Standardised Precipitation and Precipitation-Evapotranspiration Index (SPI and SPEI) with the Standardised Streamflow Index (SSI) were calculated. The influence of catchment intrinsic properties and climatic variables on the drought propagation were investigated. The results showed that although increasing evapotranspiration trends are ubiquitous, droughts in Germany are still caused by a precipitation deficit rather than higher evapotranspiration rates.

Keywords: Hydrologic drought, Meteorologic drought, SPI, SPEI, SSI, Catchment characteristics, Drought characteristics, E-OBS, Trends, Germany

1 Introduction

Drought is a recurring natural phenomenon that is developed and propagated by a deficit of the available water resources over a large area and lasting a significant time span (Dai, 2011). Other climatic variables next to precipitation controlling the variability of droughts are the temperature, atmospheric demand and heat waves (Beguería et al., 2014; Vicente-Serrano et al., 2015; Sheffield et al., 2012).

Due to its slow development, droughts have been characterised as a creeping phenomenon with a high resilience. In contrast to other natural disasters (e.g. volcanic eruptions, earthquakes) where most of the damage happens the first few hours, droughts can last many months to years and can still have impact years after the event is over (Spinoni et al., 2017). Drought is considered the natural disaster that causes most damage (Haied et al., 2017).

According to their impact, droughts can be classified into the four categories: meteorological, hydrological, agricultural and socioeconomic drought (Haied et al., 2017). Economically droughts affect all sectors and can cause severe financial damage to individuals and the state as a whole. For example the U.S. drought in the Central Plains (2012-2013) caused more than $US 12 billion (Hoerling et al., 2013) and the 1995 drought in Spain caused $US 4.5 billion damage (Guha-Sapir et al., 2004). Civil conflicts and human displacement are known to be associated with preceding drought events. With a deficit in available water for agriculture, food security can become a growing concern. The 1984 drought in Sudan affected 20-24 million people, because the crop yields only covered 20% of the demand (Epule et al., 2015). Environmentally it affects all levels of the hydrological cycle causing irreversible damage to non-resilient flora and fauna.

The analysis of drought trends has experienced a lot of scientific and public attention in recent years as the drought characteristics are changing due to climate change. Drought trends play a crucial role in the preparedness of a region for future droughts, helping to formulate mitigation plans that reduce the impact of droughts. Several studies have analysed past climate and hydrological time series resulting in different significant past trends. Dai (2011) saw an increasing trend in the percentage in global land under drought. Sheffield et al. (2012) analysed droughts over the past 60 years and came to no significant trends in drought events. Van der Schrier et al. (2006) could not differentiate between multi decadal variability and trends in the drying of the soil during summer. Analysis of the Palmer Drought Severity Index (PDSI) since 1750 by Briffa et al. (2009) showed significant positive trends in summer droughts. Spinoni et al. (2015) observed a linear increase of drought variables since 1950 in South-Western Europe. In the period 1951 - 1970 Eastern Europe, Russia and Scandinavia were drought hotspots and in the period 1991 – 2010 the Mediterranean and Baltic region were affected most by drought. The review of global drought trends from 1950 to 2008 by Dai (2011) delineates a warming up over most land areas by 1-3°C and a precipitation decrease in large parts of the world. The decreasing trend in precipitation are reflected by similar decreasing trends in runoff in the same regions. According to Samaniego et al. (2013) 35 countries will face severe water shortage by the year 2020 and by the end of the 21^{st} century Wang (2005) warned of world wide agricultural drought.

Low flow conditions, similar to drought conditions, can negatively impact river stakeholders (energy production, transport, agriculture...). In their trend analysis of 441 small catchments in 15 countries across Europe Stahl et al. (2010) found decreasing trends in the summer low flows in most regions across Europe. Steinbauer and Komischke (2016) could only detect significant trends in 33% of their catchments in southern Germany delineating both positive and negative change. In their analysis of flow quantiles in Switzerland Birsan et al. (2005) detected positive trends of the moderate and low flow quantiles during spring and autumn. During summer both, positive and negative trends are present.

The impact of drought and low water levels are easy to perceive, a deficit of water in parts of the hydrological cycle (i.e. atmosphere, soil, rivers). However, it is more difficult to understand the processes (meteorological, hydrological and biogeophysical) and their interaction leading to a drought. A mere deficit of water does not imply drought conditions, since further factors (season, climate, region, regime) need to be considered.

The concept of drought propagation is the manifestation of meteorologic drought variables into the surface and subsurface creating either hydrological and/or agricultural drought (Van Lanen, 2006). In their analysis of the relationship of meteorologic and agricultural drought Bachmair et al. (2018) found that short accumulation periods of the Standardised Precipitation and Precipitation-Evapotranspiration Index (SPI and SPEI) exhibit the highest correlation with crop vegetation stress. Barker et al. (2016) analysed the mechanisms controlling drought propagation in 121 near-natural catchments in the UK. Their results show that catchments underlain by productive aquifers feature higher correlation with longer accumulation periods of the SPI. Huang et al. (2017) analysed the propagation from meteorological to hydrological drought in an arid and semi-arid catchment in China. Their results show that the propagation time is subject to seasonal fluctuations. The results of drought propagation in the Netherlands and Spain show that quickly-responding catchments are subject to a higher frequency of minor droughts while slowly-responding catchments have a higher chance of very severe droughts (Van Lanen, 2006).

Few studies have analysed the linkage of meteorologic and hydrologic trends using standardised indicators for the quantification of the relationship. In the literature no common method to quantify the linkage of the two variables can be found. Furthermore, very few studies incorporated the influence of catchment characteristics on the drought propagation (Barker et al., 2016). Few studies have analysed the propagation time of meteorologic to hydrologic drought (Huang et al., 2017). To be able to mitigate the effects of drought and to establish a Monitoring and Early Warning system for Germany it is vital to understand the underlying process that determine the severity of hydrologic droughts. The data set used in this study has been used to analyse possible trends in groundwater levels but the linkage of the discharge to meteorologic variables was not analysed yet (Hellwig and Stahl, 2018). This study exploits the long climatic and discharge record of 337 catchments to quantify the drought propagation of hydrologic to meteorologic drought using Standardised Indices. Usually studies conduct their analysis with one climatic index only, this study will use the SPI and the SPEI to be able to distinguish between precipitation and evapotranspiration driven hydrologic droughts. Furthermore, precipitational and discharge drought characteristics and trends are calculated with the varying threshold approach of the 80^{th} percentile (van Loon and Laaha, 2015).

Although many studies have analysed discharge trends in Europe and Germany their results differ depending on the method of calculation, the data set used and the time period considered (Sheffield et al., 2012). Further studies of discharge trends give insight on possible trend changes and their seasonal and spatial variability in central Europe. This study is a further contribution to determine discharge trends in central Europe.

2 Hypothesis and goal

This study calculates discharge trends for 337 near-natural catchments in Germany and links them to observed climatic trends. Using standardised indices and the calculated trends the propagation of meteorologic to hydrologic drought is analysed. The questions addressed are:

1. Long term trends in discharge
    - 1.1. How do the analysed variables vary in time?
    - 1.2. Which catchment and climatic characteristics explain the variability of the discharge trends?
    - 1.3. Are the observed trends in line with the predicted changes due to global warming?
2. Analysis of drought propagation
    - 2.1. What are the climatic drivers of hydrologic drought?
    - 2.2. On what time scale are meteorologic and hydrologic droughts linked?
    - 2.3. Which catchment characteristics influence the drought propagation and drought characteristics?

3 Study area and data

Germany is considered a humid country with slightly lower precipitation in winter than in summer. The selected catchments (n=338) represent the climatic variation in Germany. Lowland catchments in the north under oceanic influence with a milder climatic amplitude (n= 43) and mountainous catchments with snow accumulation over winter and considerably higher precipitation (n= 29). Since in eastern Germany the data are subject to longer data gaps in the past only 27 catchments are found in the former GDR. Due to a higher station density in Southern Germany are the catchments in the North (n= 138) slightly under represented (Fig. 3.1).

For the trend analysis in this study, temperature, precipitation and discharge time series were analysed in 338 catchments. All datasets (precipitation, temperature, discharge, land use and hydrogeological information) were not obtained from the original source but from Hellwig et al. (2018) who used these data sets to analyse the impact of resolution of meteorological data sets on catchment-scale precipitation and drought studies.

The daily average streamflow data originally comes from the environmental agencies of the German federal states. Only records with no-data gaps were considered, with a continues data record from 1.1.1970 until 31.12.2009. More recent data were not readily available for all catchments. To be able to test for significant changes in Germany, the focus lie on gathering flow and climatic data for as many catchments as possible, rather than longer time series of only a few catchments. To detect anthropogenic interference visual screening was done for the streamflow data sets. This lead to the removal of one catchment, which had unrealistic changes in water flow due to the sedimentation of the gauging station. To ensure that possible trends in discharge are climate related and not dampened or amplified by anthropogenic changes, only near natural headwater catchments with a catchment size smaller than 200 km^2 were chosen. As small head catchments have a stronger direct response they are subject to less overlaying processes.

For the remaining 337 catchments temperature and precipitation were interpolated from gridded climate data (0.25° grid) of the European Climate Assessment & Dataset (E-OBS). Precipitation (as daily sum) and temperature (as daily mean) are interpolated from the E-OBS stations in Germany (Haylock et al., 2008). On average 2.4 grid cells intersect with the catchments. This data set has already been used for drought studies across Europe and for more detailed studies only in Germany (Bachmair et al., 2015; Spinoni et al., 2015, 2017).

Higher resolution data is available (e.g. REGNIE) but the objective of the study is not the detailed analysis of certain catchments, the exact timing of the drought events and the detailed deficit, rather the general trend, length and severity. E-OBS data was found to have sufficient high resolution to detect drought events (Hellwig et al., 2018).

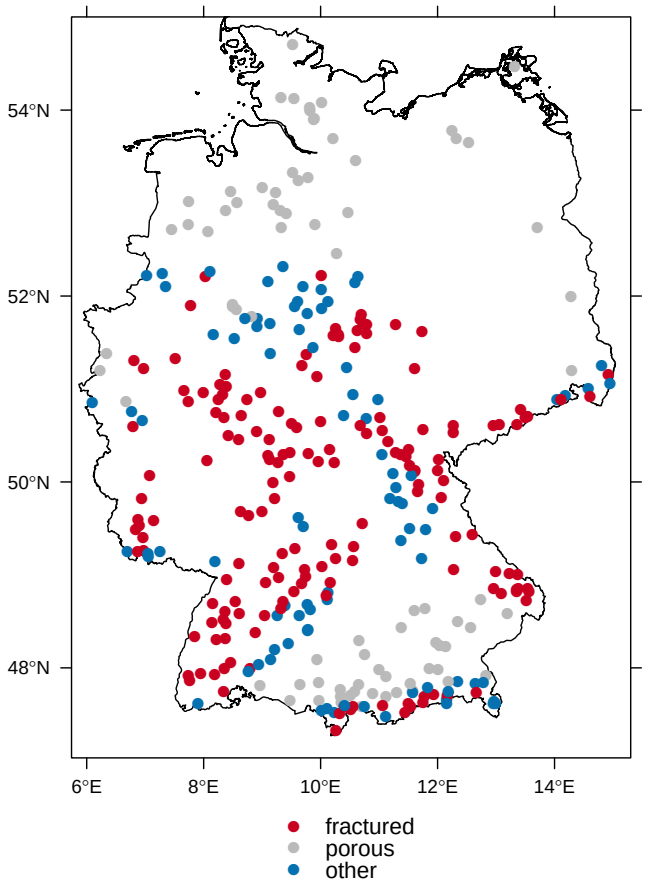

Fig. 3.1: Map of the analysed catchments with the dominant hydrogeology form.

4 Methods

To analyse drought and low flow trends in Germany trend analysis of varies streamflow characteristics, representing different flow quantiles, were conducted in section 4.1. To measure if the possible streamflow changes are driven by meteorological changes, varies climate characteristics were derived from the data sets (section 4.2). To be able to quantify the influence of monthly meteorological variation onto the monthly streamflow, standardized climatic indicators (SPI and SPEI) and the standardized streamflow indicator (SSI) were calculated for all catchments. Their calculation method is presented in section 4.3. As the magnitude of streamflow trends depend of catchment specific characteristics, these were quantified in section 4.4. As drought are defined as a deficit of the water resources over a certain amount of time, in section 4.5 the method of drought detection and quantification is presented. Trends were calculated with Mann Kendall trend analysis with correction for auto correlated samples (section 4.6). To be able to test for statistical significance of the calculated trends the significance threshold has to be corrected to incorporate the effect of cross correlation among the catchments. The chosen method to calculate field significance is described in section 4.7.

All calculations were done in R (R Core Team, 2017).

4.1 Discharge characteristics

Annual variables were calculated of the streamflow data to detect long term changes. Commonly used low flow indicators are the yearly minimum discharge of a 7 and 30 day rolling mean (Stahl et al., 2010; Coch and Mediero, 2016; Steinbauer and Komischke, 2016). To detect possible changes in other flow quantiles not represented by the 7- and 30-day rolling mean, quantile flows were calculated (Birsan et al., 2005). The following variables were calculated for all catchments:

1. 7-day-mean minimum of the summer period (May to November) referred to as Q_{min_7}
2. 30-day-mean minimum of the summer period (May to November) referred to as $Q_{min_{30}}$
3. timing (day of the year) of the 7-day-minimum occurrence referred to as T_{Q_7}
4. monthly and seasonal 10%, 35%, 50% and 80% quantile

The Q_{min_7} and $Q_{min_{30}}$ where limited to only the summer period, since a focus of this study is the attribution of discharge trends to meteorological trends in precipitation and/or evapotranspiration. During summer the catchments are dependent on their groundwater storage as the P−PET difference is negative during summer in all pluvial catchments. Therefore, the low flow of rivers mostly consists of baseflow and thus represents the long term meteorologic memory of the catchments. As higher elevated catchments have more snow accumulation during winter compared to low land catchments their yearly low flow minima can occur during winter. This would result in difficult interpretation since winter low flows could result from different meteorological effects: snow accumulation, precipitation deficit or evaporation (Stahl et al., 2010). To detect changes in snowfall patterns T_{Q_7} of nival catchments are analysed in separate analysis (Fig. 4.1).

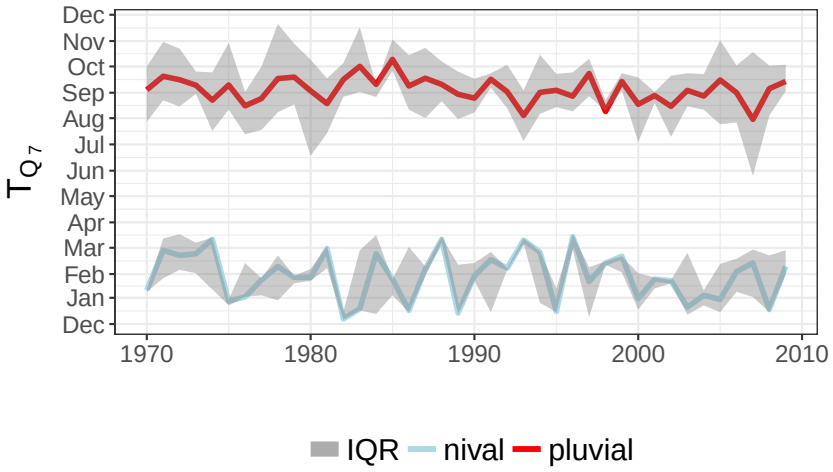

Fig. 4.1: T_{Q_7} for pluvial catchments (n=308) during summer (Mai - Nov.) and for nival catchments (n=29) during winter (Dec-Apr.). Shown is the mean (solid line) and the interquartile range.

The years in the time series are calendar years, not hydrological years. As droughts and low flows in Germany mainly occur in late summer the hydrological new year on the 1^{st} of November would split droughts occurring in October and November into two different years. Seasonal trends are calculated for the calender seasons, unless otherwise stated. Hydrologic winter period is defined as November - April, the hydrologic summmer period is defined as May to October.

4.2 Climate characteristics

As climatic variables are the drivers of the hydrological cycle, changes in climatic variables have a large influence on the discharge generation process. To determine if the observed climatic time series is subject to trends the following multiple meteorological variables were derived from the original daily time series on monthly, seasonal and annual basis.

1. precipitation (P) sums [mm]
2. potential evaporation (PET) sums [mm]
3. precipitation - PET (P−PET) sums [mm]
4. average and maximum temperature [°C]
5. number of days in the snow fall period (Dec. - Apr.) with a mean temperature below 0°C [d]
6. length of dry spells [d]
7. days without rain [d]
8. the maximum rainfall sum within 72h [mm/72h]

Variables 5. - 8. were calculated to detect potential changes in precipitation patterns. The days with a mean temperature below 0°C in the snow fall period is used to detect possible changes in which form the precipitation falls, either as rain or as snow (Birsan et al., 2005).

The climatic variable describing the length of dry spells is the yearly maximum number of consecutive days without perceivable rainfall. In the literature thresholds between 0.1 mm/d and 2 mm/d were found defining "no-rain" (Ceballos et al., 2004). Since the used E-OBS data are interpolated data subject to a larger error margin the threshold defining no rain was set to <0.5 mm/d in this study.

To detect possible trends towards more or less extreme rainfall events the number of days without rain (<0.5mm/d) and the maximum rainfall sum within in 72h is calculated for all catchments on seasonal and annual basis. Summing precipitation over 72h is a common used time span for extreme precipitation sums (Heinrich and Leibundgut, 2000).

The PET (mm/month) was calculated on monthly basis using Thornthwaite's method (Thornthwaite, 1948) since only temperature data was readily available. Other calculation methods e.g. the Penman-Monteith equation requires further variables that were not available for all catchments for the time period calculated. If the average daily temperature (T_d) is below 0, the mean is set to 0 as PET cannot be negative.

$$PET = \begin{cases} 16 \left(\frac{L}{12}\right) \left(\frac{N}{30}\right) \left(\frac{10\ T_d}{I}\right)^{\alpha}, & \text{if } T_d \geq 0 \\ 0, & \text{if } T_d < 0 \end{cases} \tag{1}$$

L is the average day length (h) of that particular month, N is the number of days in the month, T_d is the average daily temperature (°C/d), α is a correction term and I is the heat index based on the monthly mean temperature (T_{m_i}) (Thornthwaite, 1948).

$$I = \sum_{i=1}^{12} \left(\frac{T_{m_i}}{5}\right)^{1.514} \tag{2}$$

$$\alpha = (6.75 \cdot 10^{-07})I^3 - (7.71 \cdot 10^{-05})I^2 + 0.01792 \cdot I + 0.49239 \tag{3}$$

4.3 Standardized indicator calculation

In the literature a wide variety of Standardizes Climatic Indicators (SCI) can be found. The World Meteorological Organization recommends the use of the Standardized Precipitation Index (SPI) to characterise meteorological droughts (WMO, 2009). To include the effect of temperature and therefore also evaporation Vicente-Serrano et al. (2010) introduced the Standardized Precipitation Evapotranspiration Index (SPEI). The Palmer Drought Severity Index is another commonly used indice based on a physical water balance model. It could however not be used as it needs the soil water capacity as an input parameter (Palmer, 1965). In this study SPEI and SPI where calculated to quantify precipitation (P) and precipitation − evapotranspiration (P−PET) deviations respectively (Dai, 2011; Ganguli and Ganguly, 2016; Bachmair et al.,

2018).

In comparison to climatic indices it is difficult to identify a hydrological indice that is commonly used in the literature. To calculate monthly streamflow deviations the Standardized Streamflow Index (SSI) was calculated (Barker et al., 2016). The advantage of the SCIs is that their standardization allows the comparison across different catchments. To calculate the propagation of meteorological to hydrological drought, the SCIs are correlated with the SSI, allowing the attributing of droughts to either rain deficit or evapotranspirational loss. There are two different methods for their calculation: parametric and nonparametric. For this study both methods were used to calculate the SCI and the SSI.

In the parametric method a suitable probability distribution is fit to the monthly aggregated climate data using the unbiased probability weighted moments as the fitting method. For climatic variables, the intensity of the drought is dependent on the previous time step, meaning that a precipitational drought in a particular month is worse if it hasn't rained the past month either. Therefore, the SCI is calculated for different accumulated time periods. The SCI is denoted z_i for $i = 1, 2, \ldots, n$, with i representing the number of months being aggregated over (e.g. SPI-1, ..., SPI-24). The aggregation periods used in this study are 1,2,3,6,12 and 24 months to represent short term and long term climatic influence.

For every precipitation accumulation period the cumulative probability is derived based on the calculated parameters (*shape* and *scale*) from the first step. The cumulative probabilities are converted to follow the standard normal distribution (with $\mu = 0$ and $\sigma = 1$). Because the data is standardized to follow the standard normal distribution, its mean is 0 and its variation is 1 but its skewness is not removed. The SPI data tends to be skewed to the left for most catchments with few very low values, indicating months with low precipitation sums. For the SPI calculation the widely used two-parameter gamma distribution was chosen (McKee et al., 1993; Vicente-Serrano et al., 2010; Stagge et al., 2015; Ganguli and Ganguly, 2016).

SPI only considers precipitation. However, it is important to incorporate the effect of evapotranspiration as a possible meteorologic drought driver as for example the 2003 drought was caused by a severe heat wave in central Europe (Rebetez et al., 2006). Under global warming further temperature increase is expected leading to more evapotranspiration. To incorporate the possible increasing influence of evapotranspirational loss as a main drought driver it must be incorporated in the analysis of the climatic variables. To account for the effect of temperature Beguería et al. (2014) developed the SPEI, which is based on a similar calculation approach as the SPI, but extends the information content by considering the PET. SPEI is calculated from the difference between the monthly precipitation sum and the PET. The widely used log-logistic distribution was used to calculate the SPEI from the monthly P−PET values (Vicente-Serrano et al., 2010; Spinoni et al., 2017). Unlike the SPI data, the SPEI data are not skewed. SPI and SPEI were calculated in R with the $SPEI$ package (Beguería and Vicente-Serrano, 2017).

Streamflow data are subject to higher variability between the catchments than climate data. For example, an alpine river with a snow regime has a different flow behaviour than a catchment over a limestone aquifer in the north of Germany. The variability in the streamflow is the sum of many factors resulting in possible high variability of adjacent rivers. Fitting the same dis-

tribution to every month of the same catchment would mean that a low flow month with little inter annual variation would be transformed with the same distribution as a month prone to floods. Climate data, in contrast, follows a smoother interannual variation, following a similar pattern over the years. Since climate data is a macro scale phenomena adjacent catchments have a similar distribution.

Vicente-Serrano et al. (2012) recommends to fit different distribution for every month and every catchment considered. Because of the heterogeneous nature of streamflow data this would result in subjective distribution selection and a non-comparable data set which would not be reproducible. Therefore, the nonparametric method was chosen to calculate the SSI.

The nonparametric method, avoids the problem of the appropriate distribution selection by applying a normal scores transform. The monthly aggregated data are assigned ranks according to the observations of this month in the other years. The inverse normal cumulative distribution function ($\mu = 0$, $\sigma = 1$) is then applied to the ranks (Bloomfield and Marchant, 2013). The result are a normal distributed equally spaced SSI values referring to the rank with a fixed range from -1.97 to 1.97 (if considering 40 years) for every catchment. The SSI on monthly basis can be compared to the 30-day-mean flow typically used to detect annual low flows (Barker et al., 2016). Therefore, only SSI was calculated on single monthly basis and not for aggregated monthly values.

In all three indicators negative values indicate dry conditions and positive values wet conditions in relation to the mean of the considered time period over the 40 years considered. The unit of the SSI and SCI is the standard deviation of the long term mean.

To measure the propagation of meteorological drought to hydrological droughts the meteorological indices SPI and SPEI were used as descriptors of the climatic variability. As a focus of this study is the propagation of the climatic variables during drought the analysis of the propagation was limited to only drought periods. These were defines as SSI < 0. SSI below 0 indicates that the monthly streamflow mean is below the long term monthly mean. To quantify the propagation the dependence of the discharge of the meteorological variables was measured. The Spearman correlation (ρ) of the monthly SCI over different aggregation periods (n=1,2,3,6,12,24) with the SSI during drought events were calculated for all catchments. Due to the non-linear relationship between SSI and the SCI the Spearman ρ was used Barker et al. (2016). To quantify the propagation of meteorologic drought to hydrologic drought the Spearman's ρ of the SCI with SSI during drought events were calculated. To detect the influence of the emerging climate change with an accompanying potential increase in evapotranspiration changes in the linkage between the SCI and SSI during drought events were analysed. A similar approach was used by Barker et al. (2016) to calculate the propagation of meteorological to hydrological drought.

4.4 Catchment characteristics

Runoff is not only driven by meteorological variables, it depends on catchment specific discharge formation processes that vary in space and time within and between the catchments. To be

able to answer the research question of explaining the trend variability in Germany the trends were analysed in relationship with different catchment specific characteristics. The catchment characteristics analysed in this study are all considered static over time, since time varying variables were not available (e.g. soil moisture).

Because of the complex nature of discharge generation, catchment properties were derived as potential influence on the discharge generation (Table 4.1). The catchment characteristics can describe the differentiating streamflow trends that can differ in direction of change although they are subject to the same meteorological changes.

Tab. 4.1: Ranges and mean of catchment characteristics. The source of the date is noted for every variable. FEA stands of the German Federal Environmental Agencies, E-OBS are the climatic data originated from the European Climate Assessment & Dataset (Haylock et al., 2008), d signifies that the original time series was used to calculate the specific variable.

Characteristic	Range (Mean)	Unit	Data source
SR	-	-	E-OBS (d)
BFI	0.20 - 0.97 (0.62)	-	FEA
ARS	451 - 1637 (934)	mm/a	E-OBS (d)
Hydrogeology	-	category	BGR
Landuse	-	category	UBA
Catchment size	0 - 208* (88)	km^2	FEA
Mean discharge	0.003 - 9.2 (1.3)	m^3/s	FEA (d)
Mean air temperature	4.5 - 10.3 (7.9)	C°	E-OBS (d)
Long-term memory effect	0.18 - 0.79 (0.47)	-	E-OBS & FEA (d)
Latitude	-	Gauss- Krüger	FEA

* = Catchment size contains 8 catchments with no or very low catchment sizes (<5 km^2) as their actual catchment size could not be determined because the underground watershed was not definable.

- The seasonality of the low flow (SR) is a method to quantify the discharge regime. It was calculated after the method of Laaha and Blöschl (2006) from the discharge time series. It is calculated with the ratio of the mean 95% quantile of the summer months ($Q_{95_{summer}}$) and the winter months ($Q_{95_{winter}}$). Summer is defined as Mai - November and winter as December - April. Values above 1 indicate the catchment have their lowest flow in winter, values below 1 indicate it occurs in summer. In this study, catchments with their lowest flow during winter are referred to as nival and catchments with their lowest flow during summer are referred to as pluvial.

$$SR = Q_{95_{summer}}/Q_{95_{winter}} \tag{4}$$

- The baseflow index (BFI) was calculated according WMO standard (Gustard and Demuth, 2009) using the R package $lfstat$ (Koffler et al., 2016). The BFI is the ratio

of annual baseflow to the total annual run-off in a catchment. It's a widely used descriptive characteristic of catchments since it is a cumulative proxy variable for a variety of catchment properties (e.g. soil, porosity, hydrogeology,...). It's influence on drought development, propagation and length has been proven by several studies (Clausen and Pearson, 1995; Zaidman et al., 2001).

- The average rainfall sum (ARS) was calculated for the entire period 1971 to 2009 from the E-OBS precipitation dataset, providing the average rainfall sum per year of every catchment. The climatic normal periods of the German Meteorological Office (1961 - 1990 and 1991 - 2020) were not selected as the reference period, as they are partly outside of the time period available (1970 - 2009).

- The hydrogeological information of the catchments were obtained from the hydrogeological atlas of Germany (BGR, 2016). The catchments were clustered according to the dominating type of porosity: porous (n=79) or fractured (n= 170). Since catchments are usually made up of different aquifer types, the dominating (covering more than 2/3 of the catchment area) was attributed to every catchment. This resulted in 79 catchments being clustered porous and 170 being clustered fractured. Catchments with no dominating porosity were classified as "other" (n=88).

- Landuse data was derived from the harmonized land cover data set for Europe (Umweltbundesamt, 2000). The data set comes in three levels of detail, with parent categories being the most abstract and the subcategories having more detail. The parent categorization is sufficient for the analysis of hydrological processes and was therefore chosen as the descriptive land use type. The detailed subcategories would have led to 48 different categories (vs. 3 in the parent category). The land use type with the largest land cover was chosen as the land use for the whole catchment: "agricultural areas" = 194 catchments, "forest and semi natural areas" = 135 and "artificial surfaces" = 5 and 3 NAs with no land use information.

- The long-term memory effect was determined using the Spearman ρ of the discharge indicator (SSI) with the SPI-12. Catchments exhibiting a higher correlation with the SPI-12 depend more on the long term aggregated precipitation sum indicating a long term memory of the aquifer.

To explain the different magnitude of the Mann-Kendall (MK) tests the 337 catchments were analysed according to different catchment, climatic and geological categories and their spatial distribution. As an aim of this study is to explain the variance of the discharge trends the determined trends are tested if clustering helps to explain the detected variance.

4.5 Drought characteristics

Whilst minima and quantile flow values are useful flow characteristics to detect long term trend changes they do not depict information on the presence of droughts. Therefore, trends in the summer low flow (Q_{min_7} and $Q_{min_{30}}$) can not be transferred to trends in actual drought events. As one definition of droughts is the abnormal deficit in water resources, they can be defined as the deviation of the average discharge/precipitation sum at a certain time step (Dai, 2011). A drought definition method used in the literature is the varying threshold approach (Fleig et al., 2006; Van Lanen, 2006; Tallaksen et al., 2009).

In this study drought were defined using the threshold level method (van Loon and Laaha, 2015; Parry et al., 2016; Hanel et al., 2018). One common threshold is the deviation of the discharge x_i of the long term average at time step i (Parry et al., 2016). A more frequently threshold uses low flow quantiles reflecting flow characteristics (Q80, Q95) meeting ecological, navigational or energy production requirements. To identify droughts a time varying threshold is used per catchment to consider seasonal stream flow levels. The advantage of a time varying threshold over a fixed threshold is that the latter would for example not detect an abnormal low during the high water period. In this study droughts were defined if the 30 day moving average stream flow was below the 80^{th} quantile for at least 4 consecutive days. Droughts are terminated if the 30 day moving average is above the threshold.

The varying threshold approach allows the calculation of several drought characteristics for every drought event. The drought length is described by the amount of days that the variable is below the threshold. The cumulative deficit is the deviation of the streamflow data of the threshold describing the drought intensity. The deficit volumes were standardized by subtracting the mean and dividing by the standard deviation to enable comparison. The drought frequency was calculated by counting the number of drought events in every year (van Loon and Laaha, 2015).

Beyene et al. (2014) confirmed that this method is suitable for catchments with distinctive seasonality (timing of the low flow). Since in this study some catchments are found in the Alps or in the low mountain range the seasonality has to be considered. This method of drought characteristics was applied to the daily stream flow and precipitation data. For the precipitation data the 30 day moving sum was used instead of the moving average.

To measure the propagation of meteorological drought to hydrological drought, the connection between precipitation and hydrological droughts were quantified. The influence of the catchment characteristics on the drought propagation was analysed to be able to explain the drought propagation mechanisms. Trends in the drought characteristics were analysed on yearly and seasonal basis.

4.6 Trend calculation

Trends were calculated using Mann-Kendall (MK) test, which tests for the presence of a monotonic trend. The Null Hypothesis being that no monotonic trend is present. The MK test is a widely used method on hydrological studies (Douglas et al., 2000; Radziejewski and Kundzewicz, 2004; Wang et al., 2010; Wilks, 2011). Since the MK test doesn't assume that the data come

from a certain distribution it belongs to the group of nonparametric test. It has a higher power (the probability of rejecting H_0) than many other commonly used tests and it is robust against outliers (Machiwal and Jha, 2012). It is based on the sign of the difference between all possible data points $x_j - x_i$ with $j > i$. In total this would result in $n(n-1)/2$ differences. Before applying the test the data must be ordered according chronologically.

$$\begin{array}{rcrcrcl} sgn(x_j - x_i) & = & 1 & \text{if } x_j - x_i & > & 0 \\ & = & 0 & \text{if } x_j - x_i & = & 0 \\ & = & \text{-1} & \text{if } x_j - x_i & < & 0 \end{array} \tag{5}$$

To calculate the direction (positive/negative) of the trend the MK statistic (S) is calculated from all possible differences. A positive S value indicates a positive trend, meaning that the data points tend to increase with time.

$$S = \sum_{i-1}^{n-1} \sum_{j-i+1}^{n} sgn(x_j - x_i) \tag{6}$$

The variance of S is based on the number of observations (n) and on the number of tied data (g). With e_k as the number of data in the k^{th} group of tied data.

$$V(S) = \frac{1}{18}\left[n(n-1)(2n+5) - \sum_{g}^{i=1} e_k(e_k-1)(2e_k+5)\right] \tag{7}$$

Climatic data tend to underlie a certain amount of temporal dependence leading to auto correlation. The discharge or climatic variable is not independent of the preceding time step. Since this violates one of the central assumptions of the MK test, which requires the data to be independent measurements, an adjusted MK test was applied. The existence of autocorrelation can cause the false rejection of the null hypotheses (Kulkarni and von Storch, 1995). Matalas and Langbein (1962) showed that autocorrelated time series tend to larger variance than non autocorrelated ones, therefore the modified MK test has an altered method to calculate the variance. The problem of a larger variance is that the probability density function flattens, leading to a larger amount of the MK statistic (S) to fall within the critical region (Yue and Wang, 2004). Thus leading to a increased rejection rate of the null hypothesis. To avoid the issue of a large variance increasing the risk of type I error, several variance correction methods have been developed in the literature.

Von Storch (1999) introduced a variance correction known as pre-whitening. This removes the autoregressive part of a time series before the application of MK test. Yu et al. (1993) showed that pre-whiting correction method also removes part of the trend and therefore leads to a biased estimate of the trend.

Yue and Wang (2004) developed a variance correction approach based on the effective sample size (ESS). The method is based on the effect that trends (positive or negative) in a time series add to the effect of autocorrelation. Since this alters the true estimate of auto correlation, the

trend from the time series is removed before calculation of the ESS (n^*). To detrend a time series the trend slope β (equation 10) is subtracted from the data points.

$$n^* = 1 + 2 \cdot \sum_{k=1}^{n-1} (1 - \frac{k}{n}) \cdot \rho_k \tag{8}$$

where n^* is the ESS, n the actual sample size, ρ_k is the serial correlation at lag-k. n^* is not a number of observations but a fraction, describing the proportion of effective sample size. After calculating the ESS, which is based on the serial correlation coefficient at lag-k, the modified variance ($V^*(S)$) can be estimated. For all modified MK tests in this study, serial correlation at $n-1$ lags where considered for the calculation of the ESS. The modified variance ($V^*(S)$) is calculated on the basis of the ESS is and is smaller than the original variance $V(S)$. Thus reducing number of MK statistic falling within in the critical region, hence reducing the Type I error (Yue and Wang, 2004).

$$V^*(S) = V(S) \cdot n* \tag{9}$$

The modified MK test after Yue and Wang (2004) is implemented in the R package $modifiedmk$. All trends were calculated with an altered version of the function $mmky$ (Patakamuri, 2018). The p-value of the MK statistic is calculated from the two-sided Z-value on the basis of the modified variance ($V^*(S)$).

Since the MK statistic (S) only regards the sign of the differences it cannot be used to provide information about the absolute value of the magnitude of change. Therefore, Sen's slope was calculated for all trend analysis. It's calculation is based on the median of differences of all data points with $j > i$. It is a robust against outliers since it's calculation is based on the median. The value (β) indicating the amplitude of change per unit of time.

$$\beta = median \frac{y_j - y_i}{x_j - x_i} \tag{10}$$

Confidence intervals of Sen's slope (C_α) where calculated with Gilbert's Modification (Gilbert, 1987) of Theil/Sen Method with the R package $EnvStats$ (Millard, 2013). For the 95% confidence interval the calculation is based on the 95% quantile (α) of the normal distribution (Z) (Drápela et al., 2011). Since the aim of the study is to quantify environmental relevant trends the true slopes are calculated from the auto correlated time series. It is irrelevant what the magnitude of the trend would be without auto-correlation. Therefore, Sen's slope doesn't need to be corrected for it, so it's calculation is based on the MK original variance ($V(S)$).

$$C_\alpha = Z_{1-\frac{1-\alpha}{2}} \sqrt{V(S)} \tag{11}$$

$V(S)$ = variance (from equation 7)
Z = α quantile of the normal distribution

In the next step the upper and lower limits of the confidence interval are selected from the calculated quantiles M_1 and M_2 from the normal distribution.

$$\begin{aligned} M_1 &= \frac{N' - C_\alpha}{2} \\ M_2 &= \frac{N' + C_\alpha}{2} \end{aligned} \tag{12}$$

N' is the largest value of the ordered slope (β) from equation (10) (Drápela et al., 2011). The upper and lower limits of the confidence intervals are the slopes at the quantiles M_1 and M_2+1. If M_1 and M_2 are not integers the confidence interval is interpolated from the neighbouring slopes as Gilbert (1987) suggested.

The p-value of the MK test is used in the analysis to detect significant trends, Sen's slope is used to estimate the magnitude of change and the confidence intervals are used to indicate the uncertainty.

4.7 Significance

Because the catchments of the studied area are found within a similar climatic regime, the climatic and discharge time series are expected to exhibit cross correlation. This effect, known as the multiplicity problem, leads to dependence of the data points violating the assumption of independence (Wilks, 2011).

If cross correlation exists between to two data points then the underlying statistic will be correlated too. The spatial dependence of two data points can lead to higher risk of Type I error (false rejection of the H_0) at one point if at another point the Type I error has already occurred (Wilks, 2011). The actual number of effectively independent measurement points is smaller than the actual sample size $N' < N$. To correct for this it is suggested to use a modified calculation method for the lower limit of the p-value, known as field significance (Livezey and Chen, 1983; Douglas et al., 2000; Burn and Elnur, 2002).

One method of assessing field significance is the resampling method. Through a bootstrap procedure, the influence of cross correlation between the data points is determined. The bootstrap procedure is shown to produce an adequate estimate of the field significance (Renard et al., 2008)

The original time series is bootstrapped, to produce 600 resampled time series of the same length as the original time series. The MK Test is applied to each of the resamples. The percentage of stations that are significant at local significance level is calculated for all resamples. This leads to a distribution of percentages of stations being significant at local significance level. The field significance is the n-th quantile of the generated distribution. The n-th quantile is known as global significance. In this study statistical significant trends are always referred to at field significance level. The local significant and global significant level is set to 0.05.

To test significant differences between to subsets of the data either the t-test or if the assumption of normality could not be fulfilled the more conservative nonparametric wilcoxen ranked test was applied. The upper bound of acceptable p-value is the field significance value of the considered variable.

All linear regressions are conducted with normalized data, based on ordinary least square and r^2 values always refer to the adjusted r^2.

5 Results

5.1 Summer low flow

The results of the MK test and Sen's slope trend analysis of the summerly low flow characteristics show a slight tendency towards negative trends (Table 5.1). T_{Q_7} shows a stronger negative trend than the low flow variables $Q_{min_{30}}$ and Q_{min_7}. The calculated field significance value is 0.07 for all three variables.

Tab. 5.1: Percentage of catchments with significant (s) and non significant (ns) summer low flow trends (percentages always given as % of all 337 catchments). Range of the Sen's slope given for all (incl. non significant) catchments and is denoted as % change of the long term average discharge (1970-2009).

	positive		negative				
	ns	s	ns	s	range		unit
$Q_{min_{30}}$	41	19	59	35	-45	34	$\%/40a$
Q_{min_7}	41	20	59	38	-44	33	$\%/40a$
T_{Q_7}	23	10	73	51	-83	73	$d/40a$

The low flow characteristics Q_{min_7} and $Q_{min_{30}}$ do not show a clear tendency of trend direction. The T_{Q_7} on the other hand is dominated by negative trends, meaning that it has been shifting to an earlier date in 73% of the catchments over the 40 years analysed.

5.2 Spatial variability of discharge trends

No recognisable pattern can be seen in the spatial distribution of the summer low flow trends (Fig. 5.1). The heterogeneity of the low flow trends cannot be explained through their location within Germany.

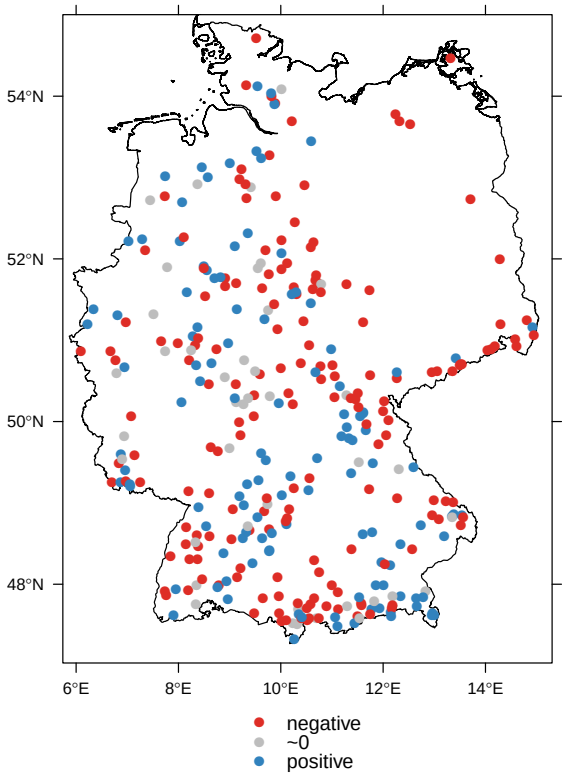

Fig. 5.1: Map of all (incl. non significant) $Q_{min_{30}}$ trends in Germany and their direction. Zero trends are defined as trends with less than ± 1% change of the long term average discharge in the years 1970 - 2009.

5.2.1 Hydrogeology

Hydrogeology is one of the BFI determining variables (Bloomfield et al., 2009). The BFI is significantly lower in karst aquifers than in porous aquifers. The BFI has no variance reducing effect on summer low flow trends. Hydrogeology, which is closely linked to the BFI, however, does exhibit an influence on T_{Q_7}. In porous aquifers is T_{Q_7} significantly (p= 2.61e-06) higher than in karst aquifers. Dividing the data into three different hydrogeological groups significantly reduces the unaccountable variance of T_{Q_7} by 12%. Porous catchments have a much higher variance and a lower number of observations than fractured aquifers (Fig. 5.2).

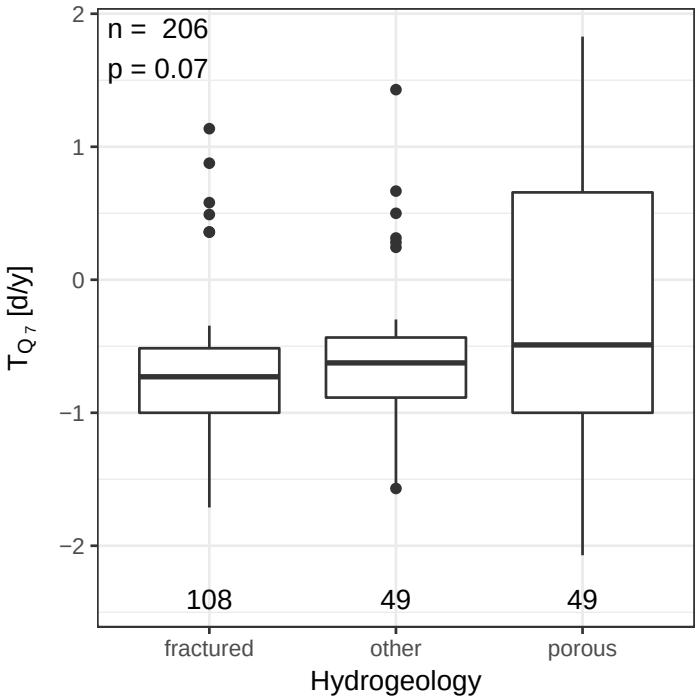

Fig. 5.2: Significant T_{Q_7} trends within different hydrogeological clusters. Numbers of observations shown at the bottom of each group. A swarm plot can be found in Fig. A.8 in the appendix, because the underlying distribution of the observations is not deductible from the boxplot.

5.2.2 Seasonality

Seasonality is the expression of the climatic condition on the streamflow regime. Considering only significant slopes of $Q_{min_{30}}$ a Wilcoxen test can confirm that the mean of nival and pluvial catchments are significantly different (p-value = 0.029). The mean slope of nival catchments is 0.005 $m^3/s/a$ and -0.001 $m^3/s/a$ in pluvial catchments. Dividing the significant $Q_{min_{30}}$ trends according to their regime significantly reduces the unaccountable variance by 12%. However, the variance is very large among nival catchments compared to the pluvial catchments. Additionally, the number of significant observations (n=18) in nival catchments is low (Fig. 5.3).

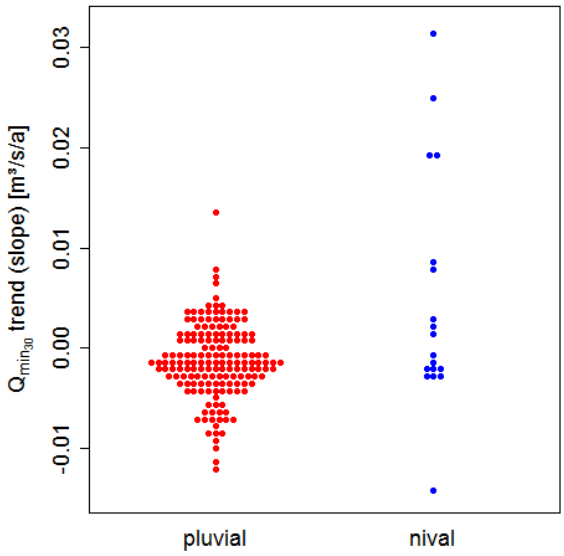

Fig. 5.3: Significant $Q_{min_{30}}$ Sen's slope grouped by their discharge regime. Every dot marks one catchment.

5.3 Seasonal variability of discharge trends

Median monthly runoff trends exhibit a clear seasonality (Fig. 5.4). Nival and pluvial catchments are examined separately, because they are under the influence of different climatic conditions. In most catchments the discharge exhibits positive trends during the winter months. Between March and April a turnover can be seen in pluvial catchments. The trend shifts from positive to negative and reaches its minima in May/June. In nival catchments the shift from positive to negative trends occurs one month later between April and March and reaches its minima in June. Dividing the data set into their regime type signifacntly reduces the unaccountable variance by 20% - 30% in all month except the winter months and May.

The analysis of further flow quantiles shows that the larger the flow quantile, the larger is the range of the monthly trends (Fig. 5.5). In spring, especially in March, all quantiles exhibit positive trends, in April a shift towards negative trends is detected. The summer period is subject to negative trends. In autumn the high glow quantile (Q_{80}) shows positive trends whilst the lower flow quantiles exhibit no trend.

A multiple linear regression was calculated between the June and March trend slopes to measure the influence of the snow melting process in nival catchments. Only catchments with trends at field significance were considered. As the seasonality (winter or pluvial) has a significant interaction, a linear model was fitted for both groups separately. Cook's distance was used to identify highly influential data points. In total 11 catchments (2 nival and 9 pluvial) were removed, as their cooks distance was higher as the recommended threshold of $4/n$ (Carsten F. Dorman, 2012).

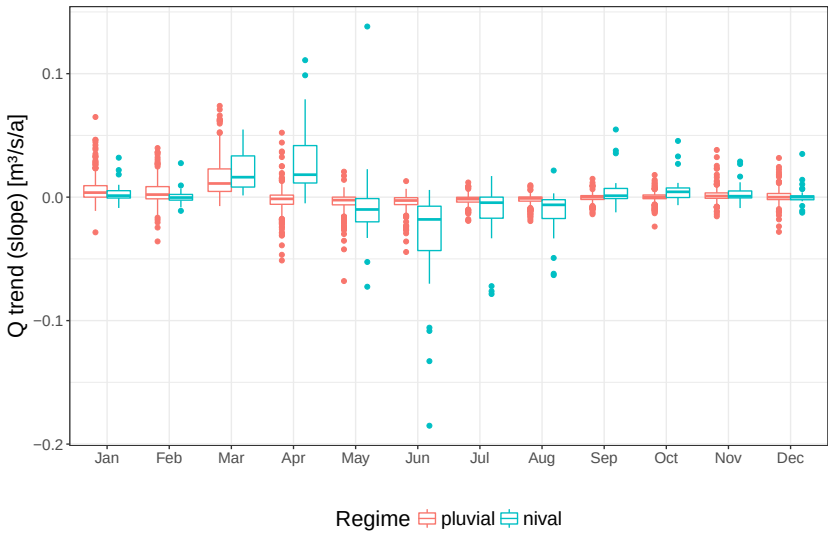

Fig. 5.4: The Sen's slope of the monthly median discharge (Q) trends of all catchments. Marked is the median and the inter-quartile range (IQR). Data points beyond the IQR are plotted individually.

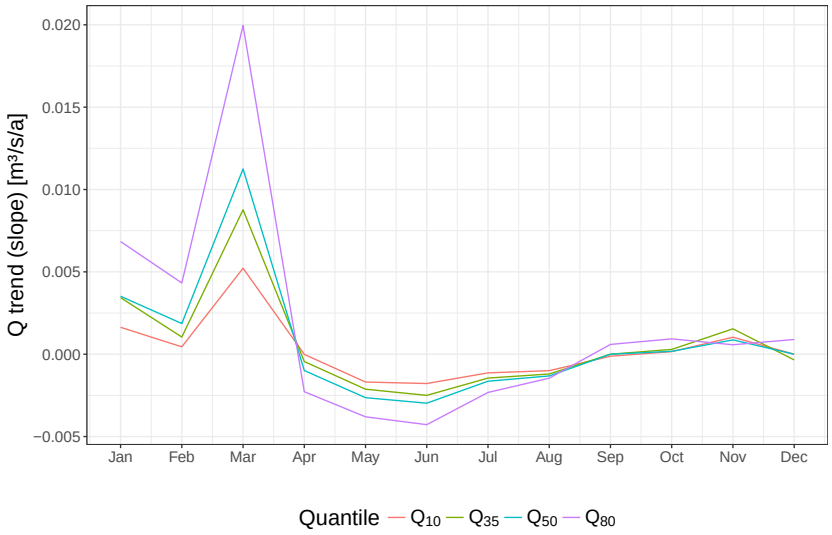

Fig. 5.5: Monthly quantile discharge trends (median of all catchments). The data is grouped according to their regime.

Most catchments have a positive trend in the mean discharge in March and a negative trend in June (Fig. 5.6). Significant positive trends in discharge can only be found in March. In the winter months leading up to March less trends in the nival catchments are significant or they exhibit both positive and negative trends at a much lower magnitude (range: December - February: -0.027 - 0.029 $m^3/s/a$ vs. range in March: 0.002 - 0.085 $m^3/s/a$). The results are similar in pluvial catchments; least significant trends in December, similar amount of significant

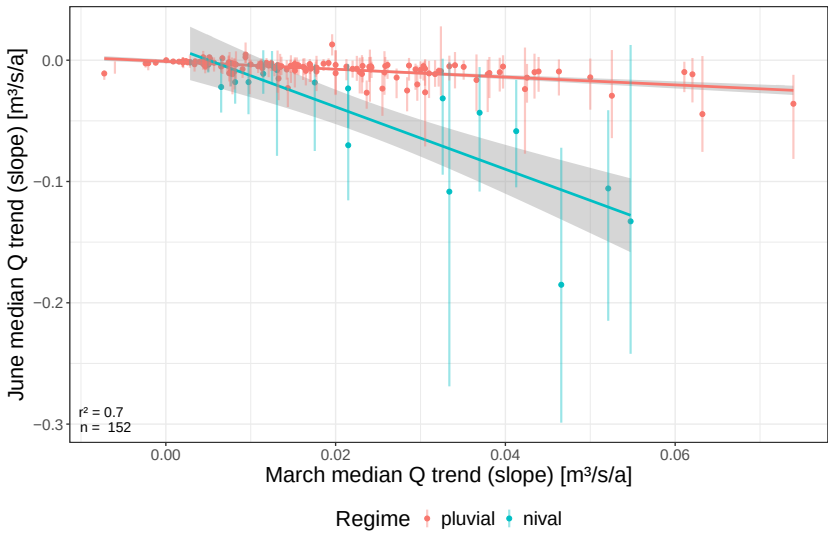

Fig. 5.6: Multiple regression of the monthly median discharge trends (Sen's slope) of March and June in nival and pluvial catchments. Only catchments with field significant trends ($\alpha = 0.03$) were used for the linear regression.

trends in January and February and March shows the most significant trends with 88% positive trends. Nival catchments depict higher uncertainties than pluvial catchments.

5.4 Meteorological trends

Because they are a main driver of the water cycle, trends in meteorology were calculated to explain the variability of the discharge trends. If all catchment attributes are static with no anthropogenic alteration, the change in discharge must come from climatic forcing. The three meteorologic variables temperature, precipitation and P−PET were analysed on a yearly and seasonal basis.

5.4.1 Temperature trends

The yearly mean temperature shows a significant increasing trend (mean: 1.5°C/40a) in all catchments (Fig. 5.7).

The monthly temperature trends show the highest increases in spring. In summer (Jun.- Aug.) temperature trends are similar for all three months. Towards the end of the year temperature trends decrease, reaching their minima in December (Fig. 5.8). To verify the strong temperature trend increase between March and April the two separate months were analysed graphically (Fig. A.2 and A.3 in the appendix).

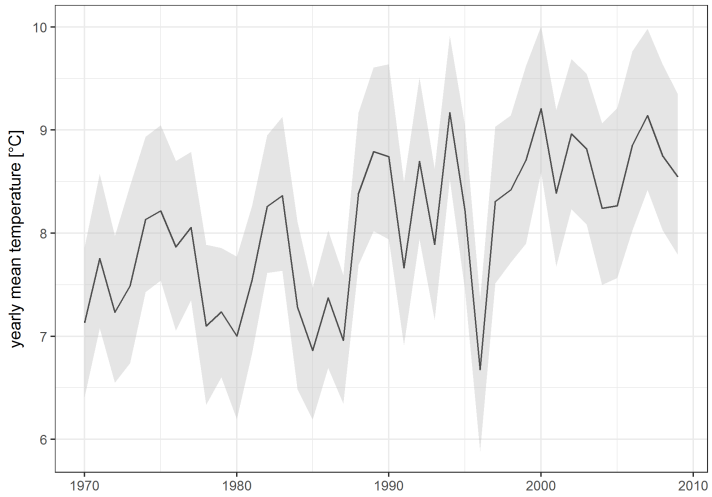

Fig. 5.7: Yearly mean temperature of all catchments, the inter quantile range is shown as shaded area.

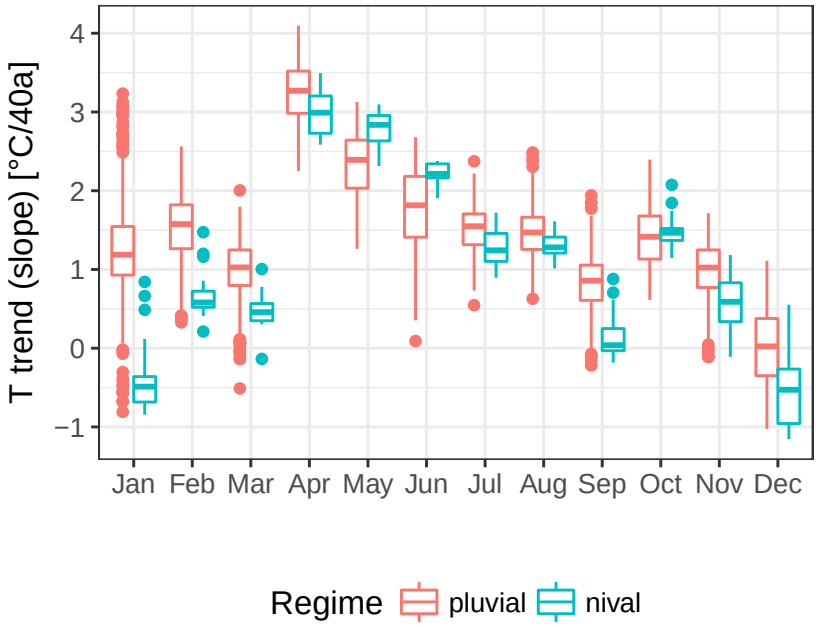

Fig. 5.8: Monthly temperature (T) trends of all catchments (all including non-significant).

Nearly all catchments experience a significant mean winter (Dec. - Feb.) temperature increase (Table 5.2). Nival catchments feature a significant (Wilcoxen Text, p-value < 0.03) lower temperature increase during spring, autumn and on a yearly basis than pluvial catchments. The calculated field significance level is 0.03 for all variables.

To quantify changes in snow accumulation trends in the number of days with a mean temperature below 0°C during the extended winter period (Dec. - April) were calculated (referred to days below 0°C in Table 5.2). The observed trends in days below 0°C are mainly negative, reflecting the observed temperature increase during winter and spring.

Tab. 5.2: Percentage of catchments with significant (s) and non significant (ns) mean seasonal and annual air temperature trends. Percentage always given as % of all catchments. Range of the Sen's slope is given of all (incl. non significant) catchments.

	positive		negative				
	ns	s	ns	s	range		unit
winter	95	53	5	0	-0.8	1.6	$°C/40a$
spring	100	100	0	0	1.2	3.2	$°C/40a$
summer	100	100	0	0	0.8	2.4	$°C/40a$
autumn	100	79	0	0	0.0	2.0	$°C/40a$
annual	100	100	0	0	0.8	2.4	$°C/40a$
days below 0°C	3	0	88	38	-18	5	$d/40a$

The winter temperature trend increases significantly with the latitude of the catchment if only non-alpine catchments. This is a useful subset, because alpine catchments, which are all found in the south, would distort the latitude-winter temperature relation (Fig. A.5 in the appendix).

All catchments feature a significant mean summer temperature increase. The summer mean temperature increase is highest in southern Germany and decreases significantly with increasing latitude. The regression of the mean temperature with the latitude is weaker during summer ($r^2 = 0.08$) than during winter ($r^2 = 0.47$).

To quantify the effect of the time period considered, the temperature trends were calculated for two different time periods: 1970 - 2009 and 1950 - 2015 (Table 5.3). Temperature was chosen as a surrogate variable as the data of the extended time period were readily available. The calculated temperature slopes of the two time periods considered are significantly different (p-value $<$ 2.2e-16) on an annual and seasonal basis (except winter, p-value = 0.047).

Tab. 5.3: Temperature trend slope ranges in $°C/5a$ for two different time periods.

	1970-2009		1950 - 2015	
	range		range	
winter	-0.05	0.25	0.05	0.15
spring	0.15	0.35	0.10	0.20
summer	0.10	0.30	0.05	0.20
autumn	0.05	0.25	0.00	0.10

5.4.2 Precipitation trends

Most catchments show a slight yearly precipitation sum increase. The yearly precipitation sum is subject to high inter annual variation (Fig. A.1). Regarding the seasonal precipitation trends, most catchments experience an increase during autumn, winter and spring. No clear trend tendency is detectable during summer. Nival regimes have significantly higher (Wilcoxen Test: p = 1.6e-10 field significance) precipitation trends during spring than pluvial catchments. On the other hand, pluvial catchments show significantly higher trends in summer and winter (p = 3.9e-06 (summer), p= 0.001 (winter)) than nival catchments (Fig. 5.9).

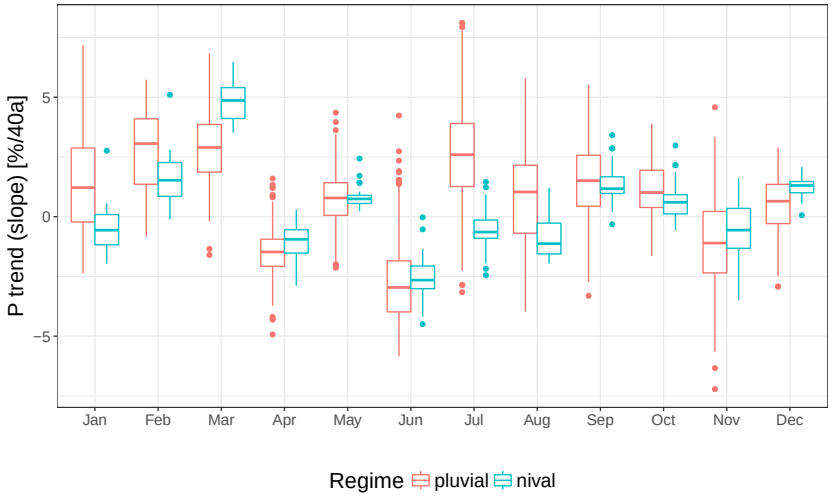

Fig. 5.9: All (incl. non significant) precipitation (P) trends on monthly basis given as % change of the ARS.

Most catchments experience negative trends in days without (<0.5mm/d) rain (dwr). Only during spring a slight majority of catchments experience positive trends (23% show significant positive trends), but also 36% of the catchments show no trends.

In the maximum amount of precipitation that falls within 72h most winter and spring exhibit positive trends. During summer and autumn the catchments exhibit in similar amounts positive and negative trends, with no clear tendency (Table 5.4).

The ranges of Sen's slope reflect the trend direction shown in Table 5.4. Spring shows the largest increase of precipitation, the 72h extreme precipitation sums and in days without rain (Table 5.5).

The detected precipitation trends are subject to very high uncertainty (Fig. 5.10). The winter precipitation trends show similar uncertainty (Fig. A.6 in the appendix). In contrast to summer are the winter trends distinctively positive.

Tab. 5.4: Percentage of seasonal and annual precipitation trends. Values are given as % of catchments that show a trend (incl. non-significant trends). As catchments possibly do not delineate any trend, the variables do not always sum up to 100%.

	Winter		Spring		Summer		Autumn		Annual	
	+	-	+	-	+	-	+	-	+	-
precip.	77	23	76	24	55	45	61	39	79	21
72h	77	23	89	11	42	58	52	48	75	25
dwr	9	53	44	20	9	64	10	72	12	75
dry spells	-	-	-	-	-	-	-	-	20	78

Tab. 5.5: Ranges of Sen's slope (of all trends incl. non significant). The range of the precipitation trends are given as percentage change of the average yearly (ARS) and seasonal rainfall sum.

	Winter		Spring		Summer		Autumn		Annual		unit
precip.	-33	47	-18	52	-21	39	-24	43	-9	39	$\%/40a$
72h	-12	17	-11	23	-20	21	-29	16	-21	21	$mm/40a$
dwr	-9	4	-6	10	-10	4	-10	6	-25	8	$d/40a$
dry spells	-	-	-	-	-	-	-	-	-58	43	$d/40a$

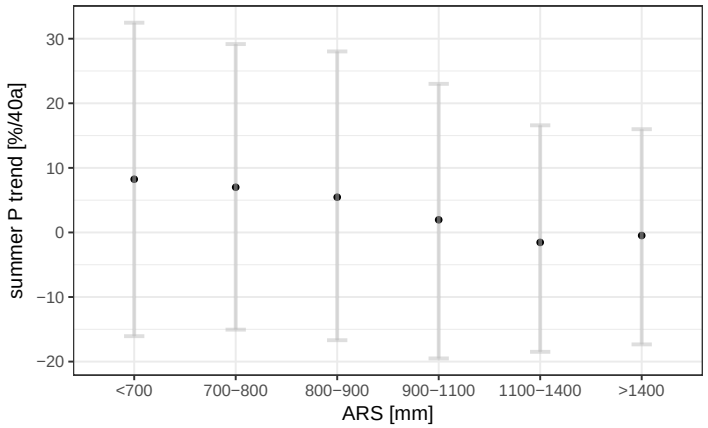

Fig. 5.10: Summer precipitation trends of all catchments grouped according to their ARS. Values are % change of the average rainfall sum during summer. Shown are Sen's slope mean and the 95% confidence intervals of every group.

5.4.3 P−PET trends

One important component of the complex discharge generation process is evaporation that acts as a reduction of the precipitation sum potentially available for discharge. The yearly course of the mean P−PET balance shows a clear seasonality (Fig. A.4 in the appendix). In nival catchments the balance is positive for all months. In pluvial catchments the balance becomes

negative in spring and summer.

As PET is based on the monthly temperature, PET trends are similar to the temperature trends (Fig. 5.8), with a strong positive increase in April reflecting the high temperature trends (Fig. A.9). Monthly trends of the P−PET balance shows that during spring and summer the monthly trends are mainly negative. During winter the trends are near 0 mm/a or slightly positive.

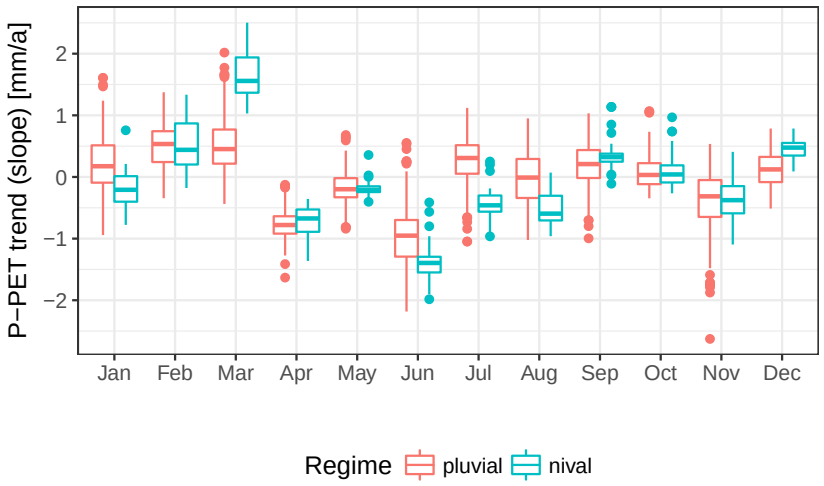

Fig. 5.11: Monthly P−PET trends of all catchments (incl.non significant trends). The catchments are split according to their regime.

5.5 Drought propagation

5.5.1 Precipitation and discharge droughts

The days of drought and drought deficit show a similar course but different amplitudes. The intensity of drought does not necessarily have an influence on the drought length and vice versa (Fig. 5.12 and 5.13). The length of droughts show mainly negative trends in both precipitation and streamflow droughts (Table 5.6).

The accumulated deficit shows mainly negative trends. The precipitational drought characteristics show clearer negative trends compared to the streamflow droughts. Comparing the 2003 drought to the droughts in the 70s, shows that the accumulated deficit in the 70s was much larger.

Drought frequency depicts mainly negative trends. However, more than half of the catchments show no trends in precipitation and streamflow droughts.

The average drought length of a catchment correlates with the BFI. The higher the proportion of baseflow, the longer are the mean droughts. For catchments with a low BFI (<0.6) this im-

Tab. 5.6: Percentage of catchments with significant (s) and non significant (ns) drought characteristic trends for both precipitation and streamflow droughts. Percentage always given as % of all catchments. The calculated field significance value is 0.03 for all catchments.

	Precipitation				Streamflow			
	+		-		+		-	
	ns	s	ns	s	ns	s	ns	s
Length	4	0	95	71	32	10	52	22
Deficit	2	0	98	63	23	7	63	15
Frequency	1	1	47	46	15	12	30	25

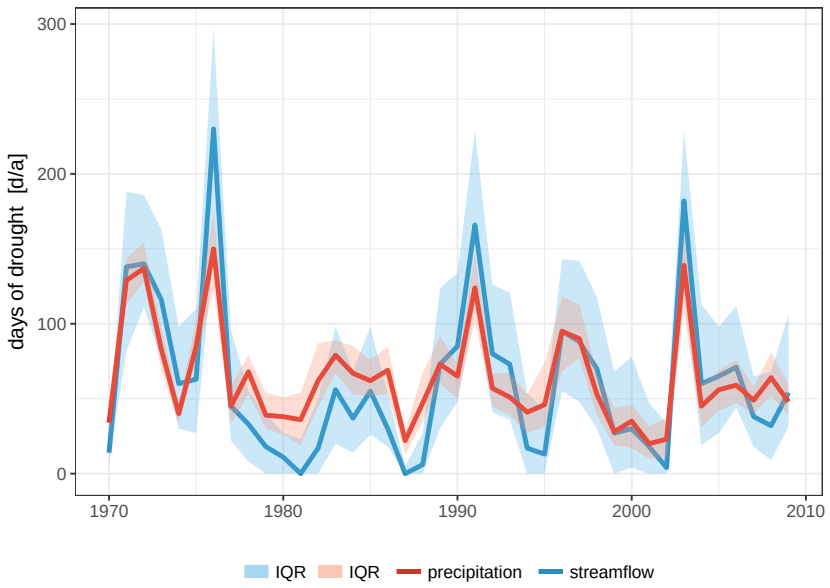

Fig. 5.12: Length of precipitation and streamflow droughts. Denoted is the median length of all catchments, the interquartile range (IQR) is shown as the shaded area.

plies that the drought length is dependent of the ARS, as their aquifers have a lower discharge buffering effect (Fig. 5.14).

Drought characteristics were calculated for two separate time periods, because severe droughts have a high leverage on the trend calculation. This highlight the influence of the time period considered when calculating trends (Table 5.7). The result shows that the droughts in 70s have a large influence on the drought trend direction. In the time period 1970-1999 the negative trends dominate, while in the years 1979 - 2009 the positive trends dominate.

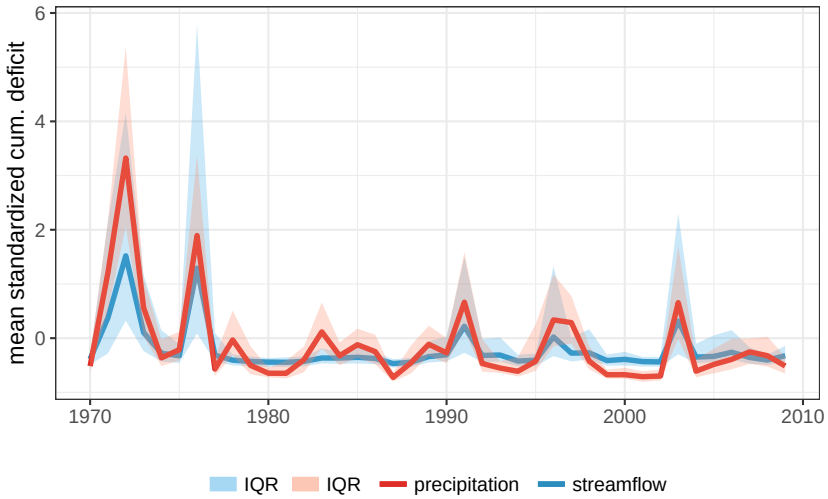

Fig. 5.13: Standardized cumulative deficit during drought events of all catchments. Denoted is the median of all catchments and the IQR. As the values are standardized for each catchment negative values are possible.

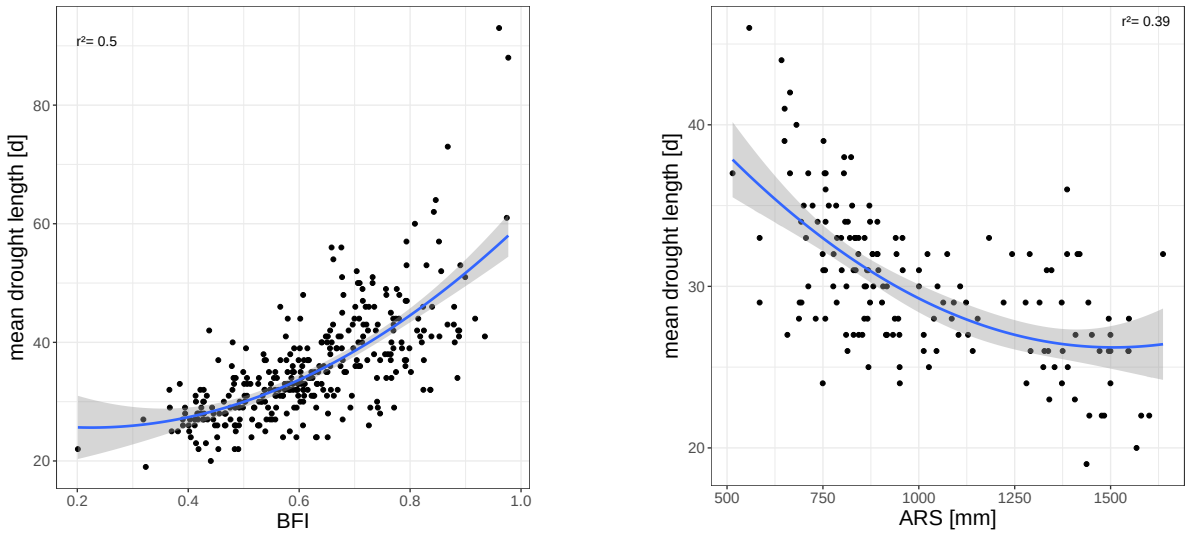

Fig. 5.14: Quadratic regression between BFI (left) and the ARS of catchments with a low BFI (<0.6) (right) with the mean drought length of all catchments.

Tab. 5.7: Percentage of catchments with significant or non significant trends.

	positive		negative	
	ns	s	ns	s
1970 - 1999	20	3	63	12
1979 - 2009	72	40	14	3

5.5.2 From meteorological to hydrological drought

As hydrologic drought events are a translation of meteorologic signals, the emergence of drought can be attributed to either precipitation deficit or above average evapotranspiration (or a combination of both). A simple visual inspection of the effect of temperature and P−PET reveals that both climatic variables are coherent with individual peak events (e.g. 1976, 1981 and 2003) of the low flow characteristic (Q_{min_7}). However, for some years (e.g. 1994) no visual connection can be drawn (Fig. 5.15).

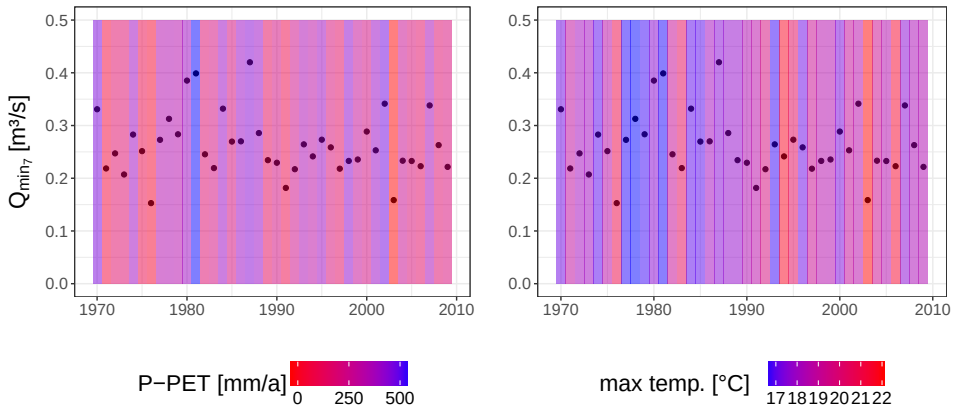

Fig. 5.15: Yearly Q_{min_7} value shown in relation to the yearly P−PET (left) and the maximum temperature (right). For both variables the median of all catchments is shown.

The attribution of streamflow droughts to either SPI or SPEI reveals that both indicators exhibit similar predictive power. Spearman's ρ of SPI and SPEI with SSI are only significantly different for the two-months aggregation period (Wilcox test, p=0.026). The 2-/3- month aggregated SCI reveals the highest correlation with the SSI (Fig. 5.16). the correlation between SSI and SCI decreases remarkably for all catchments, when SCI is aggregated over more than 6 aggregation months (Spearman's ρ: SPI-3 0.41, SPI-24: 0.21).

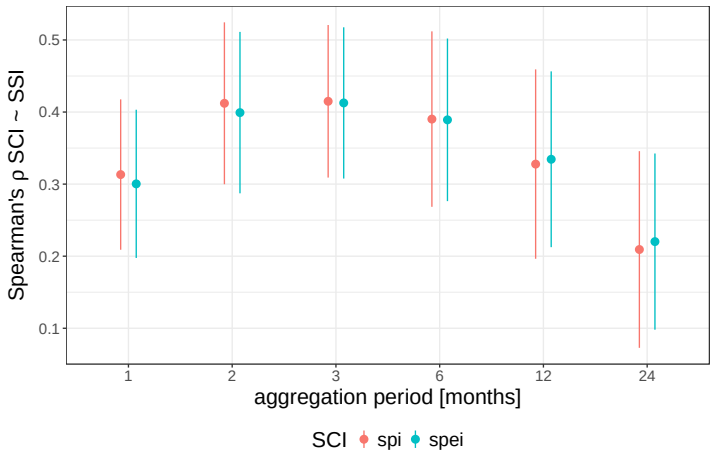

Fig. 5.16: Spearman's ρ of SPI and SPEI with SSI during drought (defined as SSI <0) for multiple aggregation periods. Shown is the mean (μ) all catchments and the standard deviation $\pm\mu$.

Catchments with low ARS ($<$700mm/a) have lower correlation of the SSI with both SCI than catchments with higher ARS. Catchments exhibit stronger correlations of the SSI with the SCI with longer (6-12 month) aggregation periods as the BFI increases (Fig. 5.17).

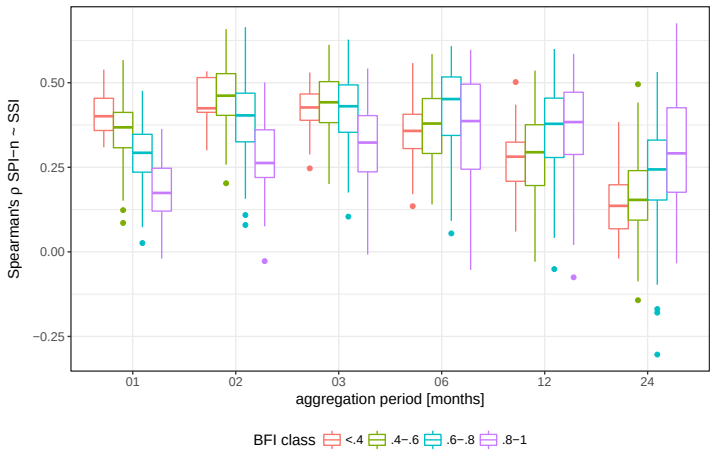

Fig. 5.17: Spearman's ρ of SPI with SSI during drought events (defined as SSI <0) for multiple aggregation periods. Correlation with SPEI-n (not shown) exhibits the same pattern and the correlation values do not differ significantly.

The amplitude of the SCI values changes over the 40 years considered. All SPEI values tend significantly (p $<$1.1e-11) towards stronger negative values. During droughts in the beginning of the time series the SPI value featured stronger negative values than the SPEI values. SPEI values depict stronger negative values in the most recent droughts (Fig. 5.18).

Fig. 5.18: Chronological course of the difference of SPI-3 and SPEI-3. Shown is the mean of all catchments.

Spearman's ρ of the monthly SSI with the SCI were calculated to analyse the seasonal dependence of streamflow on meteorological variables (Fig. 5.19). The correlation show a clear seasonality. All aggregation periods feature lower correlation during summer and higher correlation during winter. The short term aggregation exhibit higher correlation than the longer aggregation periods throughout the year.

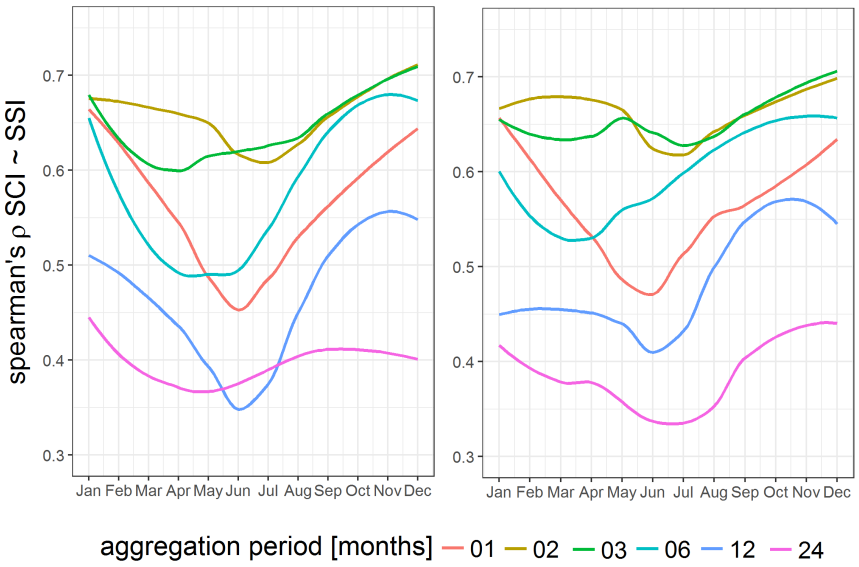

Fig. 5.19: Monthly Spearman's ρ of SPI (left) and SPEI (right) with the SSI (for all SSI values, not only during drought) for multiple aggregation periods. The yearly course of the monthly correlated values are smoothed using locally weighted scatterplot smoothing.

6 Discussion

6.1 Discharge trends

The summer low flow trends (Q_{min_7} and $Q_{min_{30}}$) exhibit a slight majority towards negative trends. However, the ranges of the trend slopes are very low (-0.01 to 0.03 $m^3/s/a$). Only when compared to the long term average discharge the low values of the slopes gain importance (Table 5.1). The summer low flow trends must therefore be handled with care as the low trend slope values are near the limit of detectability. The presented results cannot be used to draw a summer low flow trend tendency for Germany. The low flow trends reflect changes in the baseflow. The observed trends show that the climatic trends have not caused a major change of baseflow in the analysed time period.

In their analysis of the Q_{min_7} (for the whole year, not just summer) of 30 catchments in southern Germany considering the years 1951 - 2015 Steinbauer and Komischke (2016) found a slight majority of catchments exhibiting positive trends using the same Mann-Kendall trend approach. Their results show a high percentage (67%) of catchments featuring no significant trends. In this study 42% of Q_{min_7} trends are not significant. The difficulty of detecting significant trends in Germany reflects the high uncertainty of trend direction in Germany. In Mediterranean countries (Spain, Greece and Turkey) significant decreases in the low flows have been detected with the Mann-Kendall approach (Yenigün et al., 2008; Mavromatis and Stathis, 2011; Coch and Mediero, 2016)

If a trend is not significant it doesn't imply that no trend is present. No significance implies that the null hypothesis, of no trend, cannot be rejected at field significance. If a trend would exist its magnitude and direction cannot be detected with the presented method with the available data set.

To analyse the influence of the time period considered the time span was shortened to 30 years. Analysing the years 1970 - 1999 and 1979 - 2009 leads to significantly different mean Q_{min_7} trends (p-value: 0.01). This highlights the importance of always referring the detected trends to the time period analysed as the trend magnitude can differ largely in different time spans. The global air temperature experienced a drastic increase in the 80s which leads to high temperature trends if the time period analysed begins before the drastic increase (Mäder et al., 2013; Schönwiese and Rapp, 2013). The analysed time span of this study is from 1970 - 2009 as for all catchments this was the common time period with available data. An analysis of a longer time span (1950 - 2015) to calculate temperature trends revealed lower temperature trends in all seasons (Table 5.3).

6.1.1 Seasonal variability of discharge trends

To analyse the observed temporal shift in Fig. 5.4 an analysis of monthly median discharges in relation with the seasonal climatic trends was conducted for all catchments. As the climatic regime has an influence on the hydrologic regime the monthly trends were differentiated according to their regime. Monthly trends of the median are present in all catchments with general wetting trends in the winter months and drying trends in summer. Stahl et al. (2010) detected

similar wetting trends during winter and drying trends during summer in their analysis of 441 gauges in 15 European countries considering the time period 1962 - 2004.

The negative discharge trends during the hydrologic summer months (May - Oct.) are coherent with the positive temperature trends in summer leading to higher PET rates in both catchment types. Similar to the findings of this study but of different magnitude are the results of Steinbauer and Komischke (2016) who analysed temperature trends in southern Germany. In their long term trend analysis (1931 - 2015) they detected the summer half year to increase by 0.4 - 0.6°C/40a (0.6 - 2.1°C/40a in this study). Similar to the temperature increases, Germany is more frequently subject to extremely high temperatures during summer and heat waves (2011, 2014 and 2015 were among the top ten hottest years since 1881).

As the PET calculation is based on the monthly mean temperature, monthly PET trends are solely positive during the hydrologic summer months. Between March and April the PET trends are subject to a unexpected increase (Fig. A.9 in the appendix). The PET trends follow an unusual course of the year and are not coherent with the discharge trends resulting in a very low correlation with the monthly discharge values.

The analysis of the T_{Q_7} shows a clear tendency of both catchment types (pluvial and nival) to earlier onset of the Q_{min_7}. Trends to earlier T_{Q_7} in central Europe are also reported by Stahl et al. (2010). The advancing trend of the T_{Q_7} can be caused by the positive PET trends in spring leading to a shift to earlier onset of lower or negative P−PET balances (Fig. A.4 in appendix). In nival catchments the negative trends of T_{Q_7} can additionally be caused by depleting snow storage acting as a cross seasonal water storage.

Unlike the temperature trends, that are ubiquitous and positive throughout the year, the precipitation trends are not as significant and general trends cannot be deducted from the results. Only 28% (incl. non significant) of the catchments delineate negative precipitation trends (Table 5.4) during the hydrologic summer period, which stands in contrast with the negative summer discharge trends. Furthermore, the precipitation trends in the hydrologic summer period feature high inter monthly variations (Fig. 5.9) and high ranges of uncertainty (Fig. 5.10). Similar uncertainty in the summer precipitation trends are presented in the 2016 monitoring report of South Germany (Steinbauer and Komischke, 2016). Most detected trends are not significant at the significance level of 0.2 in the analysis of the time period 1946 - 2015. Moreover, the 2005 monitoring report (1931 - 1997) features different trend directions, highlighting the influence of the time period considered on the trend direction (KLIWA, 2005).

The discharge trends during winter and spring can be more easily attributed to meteorological variables. The precipitation trends show mainly positive trends (94% incl. non significant trends in the month Nov. - Apr.). The high uncertainty of the precipitation trend calculation during winter does not diminish the validity of their trend direction, since the general direction of change is positive for nearly all catchments. Steinbauer and Komischke (2016) reported a 25% increase in their trend analysis of South German areal precipitation in the winter months (Nov. - Apr.) in the time period considered: 1931 - 2010.

Temperature trends in the hydrologic winter period show mainly positive changes (95% exhibit positive trends). With a range of change of -0.8 - 1.6°C/40a. The temperature trends in spring exhibit clearer trends, as in all catchments significant positive trends were detected with a range of 1.2 - 3.2°C/40a. In their trend analysis of the years 1931 - 2015 Steinbauer and Komischke (2016) detected that the winter half year increased by 1.3 - 1.6°C/85a. The stronger temperature increase in the north of Germany during winter can be explained through positive temperature trends in the Baltic Sea. The Helsinki Commission (2013) measured that the annual mean sea-surface temperature rose up to 1°C/decade in the time period 1990 - 2008. As the influence of the temperature on the discharge during winter is different for the two types of regimes nival and pluvial regimes are considered separately.

During spring nival catchments are subject to significantly (Wilcox test, p-value: 9e-13) higher precipitation trends than pluvial catchments. However, in nival catchments it is assumed that most rain falls in form of snow, that would lead to a expected time-delayed discharge increase when the snow melts later on in the year. Since the increasing discharge trends are within the same periods as the increased precipitation trends it implies that not all precipitation falls in form of snow, but rather as rain or as snow that melts straight away. To test if in winter more precipitation falls in form of rain rather than snow the number of days in winter with the mean temperature < 0°C where analysed. The threshold of 0°C controls in which form precipitation falls (rain or snow). As the analysed nival catchments in Germany are not in very high altitudes only days with a mean temperature below 0°C during winter were analysed as during summer the precipitation usually falls in form of rain. All nival catchments experience negative trends in the number of days below 0°C (31% of nival catchments show a significant decrease) with a mean decrease of -7.6 $d/40a$ (Table 5.2). This shortens the number of days below 0°C per year and increases the amount of precipitation that falls in form of rain. Furthermore, the temperature increase in winter leads to more snow melting straight away increasing the discharge during winter.

The trend of more precipitation as rainfall is supported by the findings of Birsan et al. (2005) in their analysis of minimum temperatures during winter in Switzerland. The detected increasing trend has lead to more precipitation falling as rain. Steinbauer and Komischke (2016) have detected a lowering of the snow storage capacity in alpine areas. This has lead to 10 cm higher mean water levels in Nov. - Jan. in the time period 1990 - 2015 compared to the water levels before 1990. The analysis of European snow covers has revealed that the snow cover in March and April has been reduced by 13% and in June by 76% (European Environment Agency, 2016).

Climatological studies detected differentiating precipitation trends in the alpine area, where most nival catchments are found (27 of the 29 catchments). Brunetti et al. (2006) detected precipitation increases in winter and spring in the north-western Alps and decreasing trend in the south-eastern Alps. In this study no clear precipitation trends in nival catchments during winter can be detected. During winter only 2 catchments are subject to significant trends, most catchments have trends near 0 mm/a. This reflects the uncertainty in trend detection in the alpine region. Gobiet et al. (2014) considers the Alps as the transition zone of the European Climate change Oscillation, that acts as a barrier between the south (decreasing precipitation trends) and the north (increasing precipitation trends) and is therefore subject to large uncer-

tainty.

Nival catchments experience the turnaround of the monthly discharge trend direction in spring one month after the pluvial catchments. This is due to accumulated snow in the catchments that melts in spring acting as a cross seasonal water storage. The positive discharge trends during spring can therefore be partly attributed to an earlier snow melting process due to increasing temperature trends during spring. All nival catchments experience field significant temperature increases during spring (range: 0.06 - 0.08$°C/a$).

The earlier begin of snow melting caused by positive trends in temperature is also reflected by the earlier begin of blossom of European flowers (Menzel et al., 2006). Analysis of 25 catchments in mountainous area with a minimum record length of 40 years by Renard et al. (2008) showed a trend towards earlier snowmelt-related floods.

To investigate if the earlier snow melt causes negative discharge trends in the summer month in nival catchments the trend magnitudes of the relevant month were tested for correlation. The monthly discharge trends indicate that most snow melts during March and April. A correlation analysis between the discharge trend slopes in March and April with the slopes in May-September was conducted. The result shows that the positive trends during March and April exhibit strong inverse correlations with the months June - August (Pearson correlation: -0.6). Meaning that the increase in March and April lies within the same range as the decrease in June - August. Confirming the assumption that the negative discharge trends in summer are caused by an earlier snow melting process.

To be able to analyse the effect of the snow accumulation on the winterly low flow, an additional analysis of the low flow during winter was conducted. Nival catchments experience mainly (83%) positive trends in their winterly low flow timing with the range of -0.63 - 0.56 d/a. This can be caused through a later onset of snow accumulation, meaning that in the analysed areas snow tends to fall later in winter.

In contrast to Q_{min_7} and $Q_{min_{30}}$ trends the monthly mean trends exhibit a similar trend direction in nearly all catchments reflecting the measured seasonal climatic trends. The Q_{min_7} and $Q_{min_{30}}$ represent yearly low flow values and are therefore only subject to inter annual variations unlike the monthly flows that reflect inter and intra annual changes. The different trend magnitudes are due to the different flow quantiles that the two characteristics analyse. While Q_{min_7} and $Q_{min_{30}}$ reflect the low flow quantiles (representing roughly the 8% and the 17% quantile respectively) the monthly median represents the 50% quantile. As high flow quantiles naturally depict higher values than low flow quantiles, the high flow quantiles are subject to higher trend ranges (Fig. 5.5). Therefore, the trends in the monthly median flows are dominated by the trends in the high flow percentiles. This implies that monthly median flows are only partly useful to make a statement about changes in the low flows. Nevertheless, the detected monthly trends are represented by all analysed quantiles (10%, 35%, 50% and 80%) and imply seasonal discharge changes.

Comparing the detected climatic trends of Steinbauer and Komischke (2016) with the results of this study a clear difference in the magnitude, but not in the direction of change can be seen.

This discrepance is partly caused by the origin of the data and the time period analysed. In this study the data comes from interpolated E-OBS stations. Since the number of stations changes over time, the stations used to interpolate the areal precipitation and daily air temperature for every catchment changes over the course of the time period considered. Hence the assumption of consistency is violated for some of the catchments. However, the detected seasonal and yearly climatic trends are consistent with the direction of change detected by Steinbauer and Komischke (2016) indicating that E-OBS data can be used to detect trend directions. The unusual course of the monthly temperature (Fig. 5.8) and the monthly precipitation trends (Fig. 5.9) are possibly a product of the high uncertainty of the trends caused by the inconsistency of the data. However, precipitation exhibit little auto correlation, therefore high inter monthly variance is possible for monthly precipitation trends.

In this analysis only Thornthwaite's method of PET calculation was used. As it is a simplified calculation approach, its values cannot be transferred to environmental relevant evapotranspiration rates. Burke et al. (2006) found that in drought related studies the influence of the selected method of PET calculation has no considerable effect on the trend detection of PET. As the aim of this study was to detect trends rather than actual evapotranspiration rates Thornthwaite's calculation method was chosen, as it is based on the already available temperature data set.

6.1.2 Spatial variability of discharge trends

The spatial distribution of the $Q_{min_{30}}$ trends indicate that catchments that are adjacent to each other exhibit opposing trend directions (Fig. 5.1). Since climatic conditions are assumed to be similar in nearby catchments the different sign of the trends must be either caused by the catchments ability to buffer or amplify the climatic changes or by anthropogenic interference. The diverging trends cannot be clearly attributed to the analysed intrinsic attributes of the catchments (geology, BFI, ARS, mean temperature, discharge regime...). Since many catchment properties (e.g. altitude, soil depth, surface rock coverage, vegetation cover percentage, soil moisture) were not available for all catchments, it must be assumed that the total variance of the trends cannot be explained by the analysed variables. Consequently there must be more complex underlying processes that determine trends not captured by the data in this study.

Most catchment properties are considered static but an altering of some of the intrinsic catchment properties (e.g. land use change) can dominate the discharge trend more than climatic forcing (Kohnová and Szolgay, 2000; Groisman et al., 2001). Since in this study the trend calculation is based on the MK test, an abrupt anthropogenic induced change in discharge cannot be differentiated from a climatic induced trend. This effect was mitigated by choosing small near-natural catchments but it could not be avoided completely. It is to be assumed that some catchments are subject to anthropogenic changes such as land use change that can dampen or amplify the general low flow trends.

The only detected variable having an explanatory effect on the spatial distribution of the T_{Q_7} trends is the hydrogeology. Porous aquifers delineate a larger range of T_{Q_7}, hence in porous aquifers the summer low timing is less influenced by the hydrogeology. In fractured aquifers, the T_{Q_7} trends have a much lower variance and 63% of the catchments exhibit negative trends.

The aquifers of fractured catchments have a lower ability to buffer climatic variables. Therefore, they are subject to an earlier onset of the discharge being mainly made up of baseflow.

This study highlights the difficulty of linking precipitation trends to detected discharge trends. The heterogeneity of rainfall compared to the point measure of discharge leads to a biased quantification of the areal precipitation sum. The run-off generation is subject to a non linear translation, with many possible variables influencing the translation process. For trend analysis on a large time scale it is impossible to gather the relevant catchment properties that are involved in the run-off generation process, as these variables (e.g. soil moisture) vary in time and space. Since the primary focus of this study is trend detection and its variability, the focus lay on long time series and a large number of observations, to be able to detect trends and their spatial variability, rather than gathering long time series with the appropriate catchment properties.

6.2 Drought propagation

The characteristics of precipitational and hydrological droughts detected by the 80^{th} percentile approach follow a similar course over the 40 years analysed (Fig. 5.12 and 5.13). In the analysed time period the number of days affected by drought is larger considering streamflow than precipitation droughts. Leading to 71 $\pm$ 13 days of streamflow drought and 65 $\pm$ 4 days of precipitation drought on average per catchment and year. The number of drought events per year is smaller in streamflow droughts: on average 4 droughts per year (vs. 6 in precipitation). In their study of 44 catchments in Austria with the same 80^{th} percentile approach van Loon and Laaha (2015) found similar results of longer but rarer streamflow droughts in comparison to precipitation droughts.

During most major drought events the hydrological droughts last longer than their precipitational equivalent. Longer hydrological droughts are explainable through the manifestation of precipitation deficit in the water cycle. The return of typical precipitation sums doesn't cause streamflow in catchments to be back to mean water, since depleted aquifers need to be replenished before streamflow reverts to mean water. The longer precipitational droughts in the 80s can be explained by above average precipitation sums in 1981 (Fig. A.1) filling up the aquifer, acting as an precipitation deficit buffer. As a result streamflow droughts are shorter than precipitation droughts.

The result of the varying threshold approach for precipitation and runoff droughts are dominated by the severe droughts in the 1971 and 1976. As a result the majority of the catchments have negative trends in drought length and deficit. Similar negative trends in drought length were reported by Steinbauer and Komischke (2016) of their analysis of drought length in the years of 1951 - 2015 in South Germany (n=30). With regards to the drought frequency, most catchments exhibit no trends at all.

For all three variables (length, severity and frequency) precipitation droughts exhibit clearer negative trends than streamflow droughts. As most droughts in Germany occur during summer and autumn (June - November) the drought characteristics were considered separately in this

time period. Regarding the yearly cumulative discharge drought deficit 17% of the catchments exhibit field significant positive trends (6% negative) and 21% positive trends in days of drought per year (9% negative). The seasonal trends of the precipitational droughts exhibit a contrary magnitude of change during the same season. At field significance: 63% of the catchments delineate negative trends in days of drought per year and 60% in yearly cumulative drought deficit.

The discrepance can be explained through the non-linear transformation of precipitation to discharge. The severity and length of a streamflow drought depends on further variables than the climatic conditions. Further variables controlling the severity of a hydrologic drought are groundwater levels, soil moisture, anthropogenic interference, landuse and the preceding climatic conditions.

Trend calculation of yearly values for a short period of time results in a low number of observations (n=40). If extreme values are present it has no effect on the MK trend calculation but it does have an influence on the slope calculation as it is based on the median of actual differences and not on the sign of the difference. Therefore, for the drought characteristics calculation the slopes of the drought trends are dominated by extreme events that dominate the value of the slope. Since two major drought events were directly at the beginning of the time series considered (1971 and 1976), the drought characteristics slopes are mainly negative. This reflects the importance of the time period considered when calculating trends. If the time series would begin 1979, most drought characteristics would delineate positive trends, as the major drought events in the 70s would be left out (Table 5.7). Unlike the discharge trends that are calculated on a yearly basis drought trends are event based leading to a large bias due to individual peak events exhibiting a high leverage on the trend slope.

The results of this study reflect the drought trends of the years 1970 - 2009 but they are only an excerpt as the known recent droughts (2010, 2013, 2015 and 2018) of similar severity as the droughts in the 70s were not included in the study. The method of drought detection presented in this study can be used to compare recent droughts with historic droughts, but for trend analysis longer time periods should be considered. Briffa et al. (2009) analysed trends in moisture availability since 1750 till 2003 in Europe based on the PDSI. Their results show highly significant trends towards more frequently occurring dry summers in the most recent part of the record.

To analyse the catchment intrinsic properties controlling the drought characteristics, Pearson correlations between mean drought characteristics and catchment properties were calculated. The BFI is a proxy variable describing the aquifer behaviour. It exhibits high correlation with the mean drought duration (Pearson correlation = 0.7). As the meteorological droughts are manifested in the groundwater levels, catchments with a high BFI suffer from longer droughts, because their streamflow is stronger dependent on the groundwater storage. A depletion of the groundwater levels during drought leads to long streamflow droughts, till the groundwater levels are back to normal. As catchments with a high BFI are subject to longer droughts they have a lower drought frequency (Pearson correlation of the BFI with drought frequency: -0.72). In catchments with a low BFI (< 0.6) the drought length is inversely correlated with the ARS (Pearson: -0.6). Catchments with a high ARS suffer from shorter droughts than catchments with a low ARS because the discharge in these catchments is fed by direct precipitation rather

than groundwater baseflow (Fig. 5.14).

Analysing the drought propagation pattern in regards to catchment characteristics reveals that nival catchments exhibit significantly lower correlation of the meteorological variables (SCI) with discharge during drought (SSI). This suggests that in nival catchments further meteorologic variables not incorporated by the SPI and SPEI control the snow accumulation and snow melting process determining the discharge.

Further analysis shows that the catchments with higher BFI correlate stronger with longer aggregated SCI (6 and 12 months) than with shorter aggregation periods. (Fig. 5.17). The correlation with longer aggregation periods shows that these catchments are subject to a temporal delay from meteorological to hydrological drought. The variance of the drought propagation increases with increasing BFI for all aggregation periods. Due to the more complex discharge formation process in catchments with a high baseflow share, these catchments delineate higher variance of the drought propagation correlation.

Catchments with low ARS (<700mm/a) exhibit significantly (p-value: 7.225e-06) lower correlation of the SCI with the SSI during drought periods. In these catchments further variables describe the manifestation of meteorological to hydrological drought.

The differences between the Spearman's ρ of the SCI with SSI are only minor for all aggregation periods. The mean Spearman's ρ of all catchments with SSI is 0.48 for SPI and 0.47 for SPEI. To calculate the mean the optimal aggregation period that best describes the catchment memory was chosen for every catchment (usually 2 or 3 months). The SPEI is a correction of the SPI for the evapotranspirational loss. The similarity of the two highlights the minor influence of evapotranspiration on the hydrologic drought manifestation in Germany since this correction results in similar correlation during drought periods.

While the difference between the correlation of SPI and SPEI is negligible the correlation with different aggregation periods differs for unique drought events. Figure 5.16 shows that the two and three months aggregated SCI exhibit the highest correlation with SSI during most drought events. This highlights the general short memory of German aquifers. For some unique events the highest correlation shifts from 3 aggregated month to 6 months (in the year 1976, 1986 and 2003). The shift indicates that during these drought events a longer period of the climatic variables had to be considered to be able to quantify the extend of the hydrologic drought. However, considering all drought events the 3 month aggregated SCI exhibits the highest correlation with the SSI. No trend towards longer or shorter aggregation periods could be detected. .

The seasonal dependence of discharge of the SCI shows a clear seasonality (Fig. 5.19) for longer aggregation periods and the 1-month aggregated SCI. Both indicator types exhibit a lower correlation during summer. The 2 and 3 month aggregated SCI exhibits a lower yearly amplitude showing that these aggregation periods can be used to quantify the drought propagation throughout the year. Furthermore, the summer discharge mainly depends on the preceding precipitation sum of the past 2-3 months. The slightly lower correlation during summer of both indicator types over all aggregation months displays the lower connection of the discharge and the climatic variables during summer. This supports the difficulty of linking the detected

discharge trends to the detected meteorologic trends during summer (section 6.1.1).

The non parametric method of calculating the SSI has lead to tied values. This can have the consequence that two droughts in the same catchment but at different time steps with differentiating drought severity would have the same indicator value allocated. The parametric method would have avoided this through fitting the data to an appropriate distribution. In the literature no common distribution could be found that is usually fitted to discharge time series. Distributions that have been used are the Tweedie, Pearson-III, Gamma, Generalized Extreme Value or the 3-Parameter Log Normal distribution (Shukla and Wood, 2008; Barker et al., 2016; Huang et al., 2017). For the analysed catchments in this study the fitting of one distribution for all catchments lead to a very low goodness of fit for certain catchments. Vicente-Serrano et al. (2012) suggested to fit a distinct distribution for every catchment for every month separately. In this study the non parametric method was chosen to calculate the SSI consistently for all catchments over the whole period. The consequently loss of information for certain months was accepted for the benefit of consistency. The subjective choice of an appropriate distribution for every month in the parametric method would have made the study not reproducible. For the climatic data the parametric method provided the better results, as climatic variables showed a high goodness of fit with certain distributions. Unlike for the SSI a commonly fit distribution for the SCI can be found in the literature: Gamma for the SPI calculation and the log logistic distribution for the SPEI calculation (McKee et al., 1993; Vicente-Serrano et al., 2010; Stagge et al., 2015; Ganguli and Ganguly, 2016). This eases comparison to other studies and enables the SCI to be reproduced from the data set.

6.3 Climate change

With regards to the predicted change due to global warming the results of global circulation models (GCM) in the literature predict changes in European summer precipitation patterns and sums (Dai, 2011). Christensen and Christensen (2003) applied the high resolution model HIRHAM4 on the IPCC emission scenario A2 and B2 resulting in a projected general drying of the summer months despite of higher risks of summer floods due to increased frequency of heavy precipitation events (projection for the period: 2071 – 2100). This could lead to the phenomenon of dry summers interrupted by short floods as a possible future scenario. From a meteorological perspective more extreme events are expected due to anthropogenic forcing. The increase of green house gases leads to an increase in the moisture holding capacity, which in return leads to fewer but extremer precipitation events (Trenberth et al., 2003). As this could be a possible explanation of the drying trends in the summer months the days with no rain ($<$0.5mm) and the 72h max rainfall trends were observed.

The predicted summerly precipitation pattern change is not seen in the analysed data of this study. Considering the days without rain in summer 85% of the catchments show negative trends. In the analysis of extreme precipitation events no increase in the extreme precipitation events could be measured. The majority of the catchments (61%) feature negative trends in the 72h maximum precipitation sums during summer.

Similar findings are reported by Hundecha and Bárdossy (2005) in their analysis of extreme precipitation events in Western Germany for the time period 1958 - 2001. Extreme heavy precipitation events during all seasons but summer (June - August) exhibit positive trends in frequency and magnitude. During summer, the extreme events delineate negative trends in both magnitude and frequency. Widmann and Schär (1997) and Birsan et al. (2005) found significantly increasing intense precipitation trends (period analysed: 1901 - 1994 and 1931 - 2000 respectively) in Switzerland only for the winter and autumn months, especially in Northern Switzerland.

The observed trends in discharge and days below 0°C during winter in this study reflect the projected change in snowfall sums (Arnell, 1999). Their macro-scale hydrological model output for the year 2050 project precipitation that falls as snow to become less relevant leading to higher discharge trends during winter and decreasing trends in spring in Europe. The positive trends during winter are also observed in this study, however during spring the projected change can not be confirmed from the observed trends. This is due to the projection that outlines the climate change induced change by the year 2050, up to now the snowmelt related discharge has lead to increasing trends in spring in nival catchments.

In the literature most projected changes in discharge in the Mediterranean region exhibit negative trends. For Europe north of 50°N the projected changes are negative (Gosling et al., 2016; Marx et al., 2018) or positive (Arnell, 1999; Forzieri et al., 2013). The diverging trends are caused by the uncertainty of the model output, the model choice and the emission scenario. The observed low flow trends in Germany reflect the uncertainty of global warming induced change for central Europe. While the trends in low flow do not show a clear signal the observed seasonal changes show a clear direction of change. The projected earlier snow melt (Musselman et al., 2017) is reflected by the detected positive discharge trends during April and March in nival catchments.

In this study drought propagation was measured as the manifestation of climatic drought signals in the discharge. The selected measurement method of correlating the SSI with the SCI has revealed difficulties, as discharge during drought cannot be completely described by the climatic variables of SPI nor SPEI. Nevertheless, the results show that in Germany hydrologic droughts are precipitation rather then evapotranspiration driven. With regards to the predicted climate change in Germany it is uncertain if this drought driving balance will be maintained. Temperatures are expected to increase further and therefore the evapotranspiration proportion in the development of hydrologic droughts is expected to increase. The negative trend of the difference of SPI-3 and SPEI-3 shows that SPEI-3 values are becoming more negative than the SPI-3 values (Fig. 5.18). The increase in SPEI-3 deviation is in line with the temperature increase (Fig. 5.7). To detect if droughts are becoming increasingly caused by evapotranspiration loss, trends in the correlation of the SSI (during drought events) with the SCI were analysed. Although SPEI values are decreasing in the past no trend towards a dependence of the discharge of SPEI could be detected. Regarding precipitation, Germany is subject to uncertain predictions for the precipitation during summer, only during winter most models agree on the sign of change. These modelled predictions are in line with the observed increasing trends in precipitation during winter.

To be able to link hydrologic observations to climate change induced changes requires fingerprint methods (e.g. GCM outputs) (Hasselmann, 1993, 1998). In this study observed meteorologic and hydrologic trends are put in relation with the projected GCM outputs found in the literature. The observed trends in this study are partly in line with multiple projected changes. However, with the applied method in this study the cause of the observed trends cannot be distinguished between climate change induced or a reflection of the natural variability of the hydrologic cycle.

6.4 Further Research

To be able to understand the underlying processes controlling the drought propagation and the discharge trends further catchment intrinsic properties should be included as possible explanatory variables. The intrinsic catchment properties can explain the spatial variance of the diverging discharge trends and can therefore help to set up a drought M & EW.

Analysis of the propagation of meteorologic to hydrologic drought only incorporated the SSI as a surrogate of the hydrologic cycle. Analysis of the relationship of further hydrologic indices reflecting groundwater levels (e.g. Standardised Groundwater Index) or vegetation indices expressing the drought propagation through further levels of the water cycle. To quantify and mitigate the drought propagation along the hydrologic cycle it is vital to investigate the underlying processes controlling the drought propagation.

7 Conclusion

Changes in climatic variables due to climate change are measurable in Germany, but their hydrological implications in the form of ubiquitous negative summer low flow trends could not be detected in the analysed time period. The analysed Q_{min_7} and $Q_{min_{30}}$ low flow variables only show negative trends in 59% of the catchments. As the low flow trends reflect changes in the baseflow the unclear trends in the low flow imply that the observed climatic changes have not reached the baseflow in the analysed period.

T_{Q_7} shows advancing trends in 73% of the catchments, which indicates an earlier baseflow dependence of the discharge. Regarding the spatial distribution of the trends only hydrogeology could partly explain the spatial distribution of T_{Q_7}.

Seasonal trends must be differentiated from the yearly low flow trends that do show a clear trend tendency in almost all of the analysed catchments. This highlights the wide spread seasonal shift due to climatic forcing.

In winter and spring the monthly discharge trends exhibit clear positive trends in all considered quantiles. The increase in pluvial catchments can be attributed to the increase of precipitation sums in winter and spring. Nival catchments are only subject to significant precipitation increases during spring. During winter the trends are near 0. Therefore, positive discharge trends in spring are partly caused by positive precipitation trends and by an earlier snow melt peak through higher temperatures in spring and summer. The positve trends during winter can be explained bs a lower amount of precipitation that falls as snow, which leads to more direct discharge. The advancing of the snow melt peak has lead to negative trends in summer. As the amount of snow in nival catchments is predicted to be reduced and to melt earlier, nival catchments likely to depict negative trends during spring.

The observed drying trends in discharge during summer months could not be easily attributed to detected climatic trends. The evapotranspiration trends do not exhibit a meaningful relationship with the monthly discharge trends. Additionally, summer precipitation exhibit slightly positive trends, which stand in contrast to the detected ubiquitous negative discharge trends. These contradicting trends are to be regarded with the high uncertainty of the precipitation trend slope (Fig. 5.10) and the low number of catchments which exhibit significant (12%) summer precipitation trends.

Despite the fact that evapotranspiration increases measurably, the analysis of the propagation from meteorologic to hydrologic droughts showed that droughts in Germany are still controlled by precipitation. Furthermore, discharge in summer strongly depends on the precipitation sum of the past 2-3 months. During the other seasons the longer climatic aggregation periods exhibit similar correlations with the SSI. Catchments with a low BFI exhibit stronger correlation of the SSI (during drought) with short aggregation periods (2-3 months) of SPI and SPEI. While in catchments with a high BFI the droughts are stronger correlated with longer aggregation periods.

The detected positive trends in drought characteristics (length and deficit) during summer and autumn will cause further environmental, agricultural and economic stress already experienced in past droughts. Changing water availability requires adequate water management to reduce the impact of the detected decreasing water levels during the summer months. M&EW systems should take into account the observed seasonal shifts in discharge trends to be able to mitigate future water deficits.

Appendix

Abbreviations

Name	Unit	Symbol
maximum amount of precipitation that falls within 72h	mm	72h
significance level		α
years	n	a
Average Rainfall Sum	mm/a	ARS
Baseflow index	-	BFI
Bundesanstalt für Geowissenschaften und Rohstoffe		BGR
length of dry spells	days [d]	dry spells
days without rain	days [d]	dwr
European Climate Assessment & Dataset		E-OBS
Effective Sample Size		ESS
German Federal Environmental Agencies		FEA
Global Circulation Models		GCM
German Democratic Republic		GDR
Interquartile range		IQR
monitoring and early warning		M & EW
Mann-Kendall trend test		MK test
mean		μ
North Atlantic Oscillation		NAO
non significant		ns
Precipitation	mm/time	P
Palmer Drought Severity Index		PDSI
Potential Evapotranspiration	mm/time	PET
Precipitation − PET	mm/time	P−PET
discharge	m^3/s	Q
quantile flow	m^3/s	Q_{xx}
7-day-mean minimum of the summer period	m^3/s	Q_{min_7}
30-day-mean minimum of the summer period	m^3/s	$Q_{min_{30}}$
7-day-minimum occurrence	date	T_{Q_7}
adjusted r^2	-	r^2
Spearman's rank correlation coefficient		ρ
significant		s
standard deviation		σ
Standardised Climatic Indicators		SCI
Standardised Precipitation-Evapotranspiration Index		SPEI
Standardized Precipitation Index		SPI
Seasonality Ratio	-	SR
Standardised Streamflow Index		SSI
temperature	°C	T
Umweltbundesamt		UBA
World Meteorologic Organization		WMO

Figures

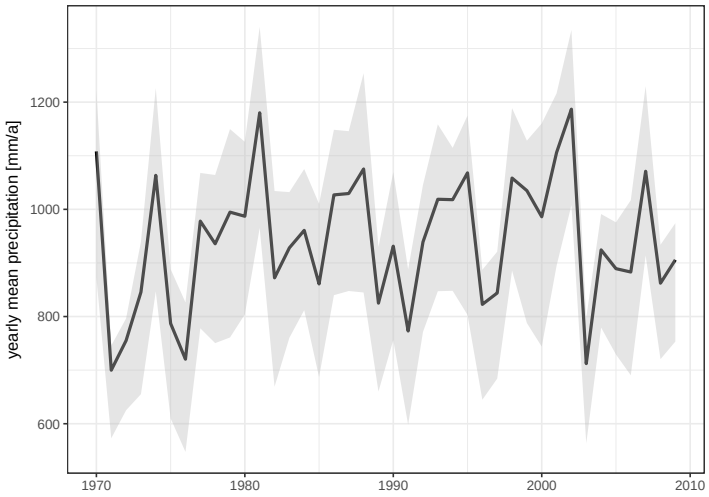

Fig. A.1: Yearly precipitation sums of all catchments. Marked is the mean (black line). The shaded area is the inter-quartile range (IQR).

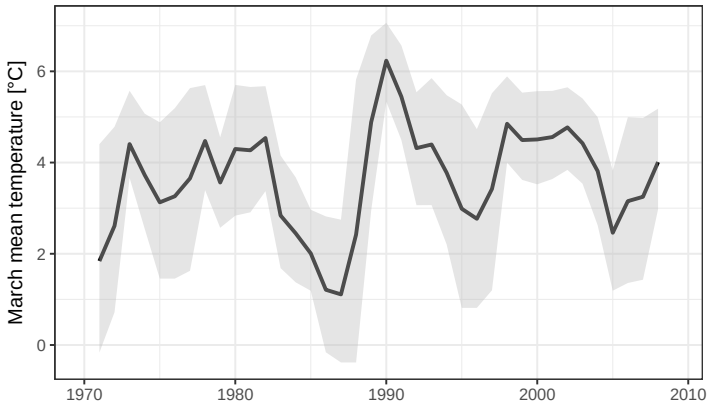

Fig. A.2: March mean temperature trend of all catchments. Marked is the mean (black line). The shaded area is the inter-quartile range (IQR).

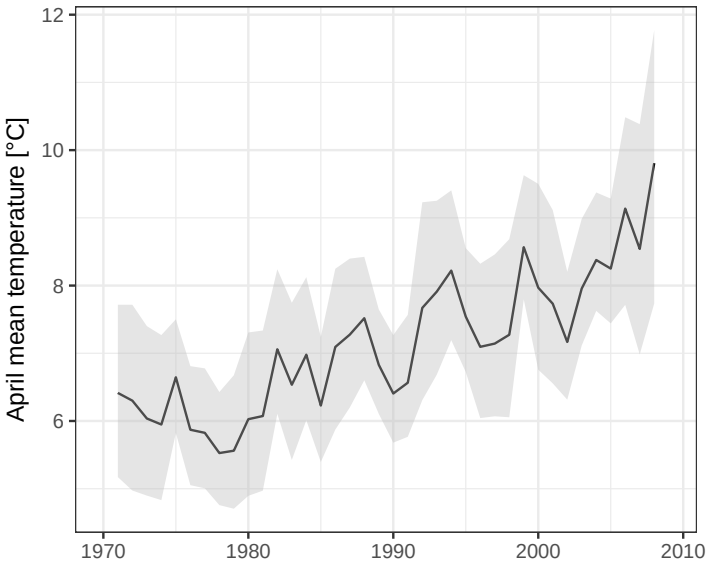

Fig. A.3: April mean temperature trend of all catchments. Marked is the mean (black line). The shaded area is the inter-quartile range (IQR).

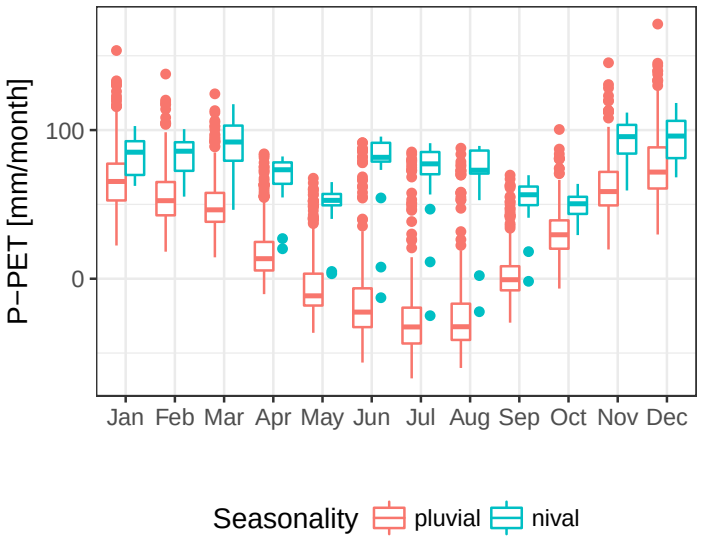

Fig. A.4: Monthly mean P−PET values of all catchments.

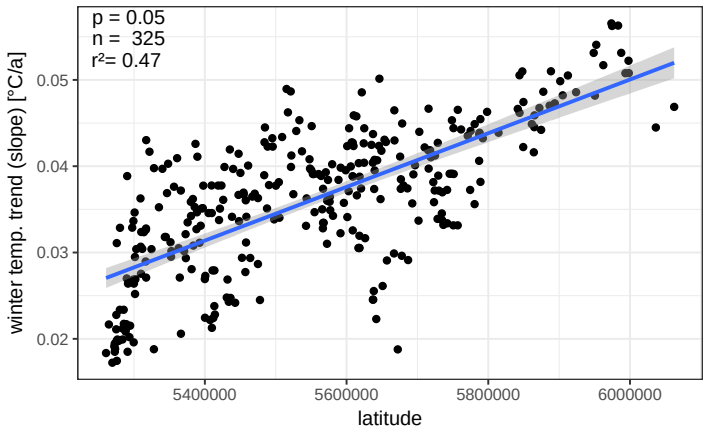

Fig. A.5: Linear Regression of the mean winter (December - April) temperature with the latitude. Only field significant trends are considered. The field significance level , the number of observations and adjusted r^2 is marked in the top left corner. Latitude is given in Gauss-Krüger coordinates.

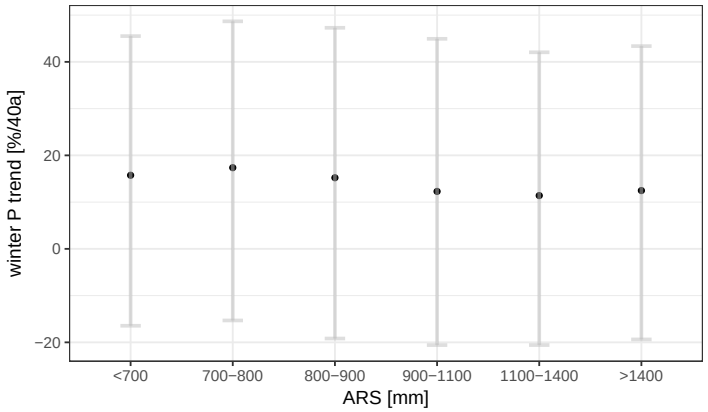

Fig. A.6: Winter precipitation trends of all catchments grouped according to their ARS. Values are % change of the average rainfall sum during winter. Shown are Sen's slope mean and the 95% confidence intervals of every group.

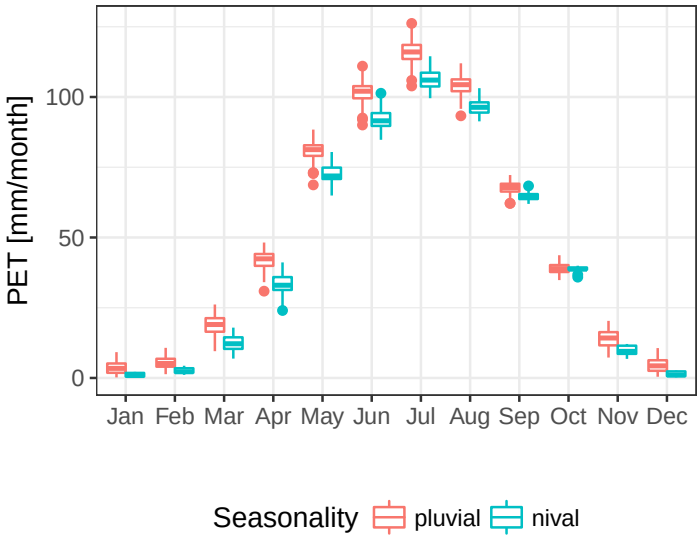

Fig. A.7: The PET values of all catchments in every month. The catchments are categorised according to their regime.

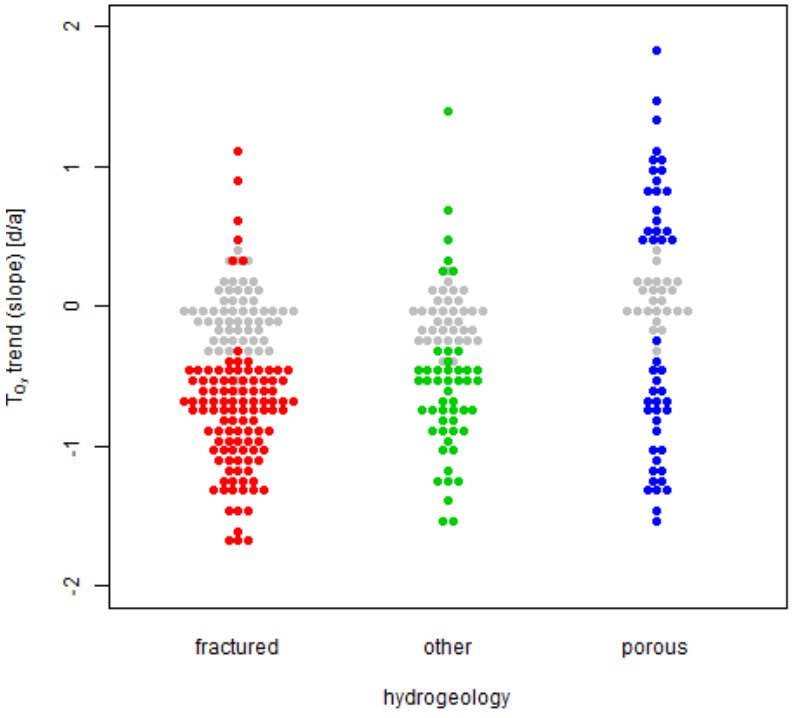

Fig. A.8: T_{Q_7} trends. Non-significant trends are shown in grey.

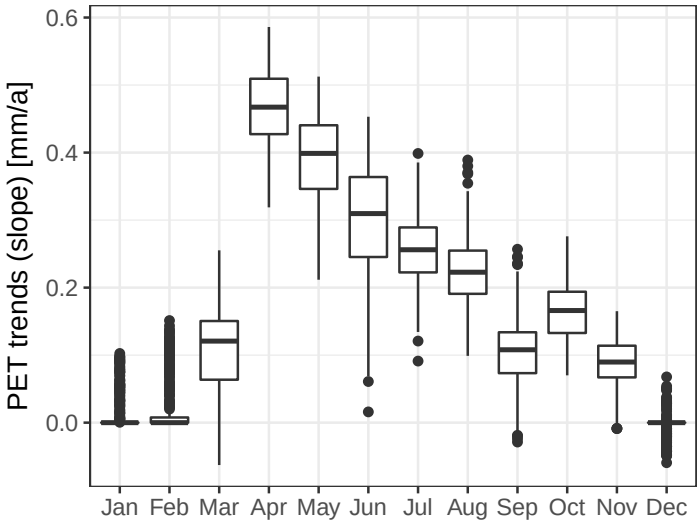

Fig. A.9: Monthly PET trends of all catchments (incl. non significant trends).

R Code

The code can be found on Github (`https://github.com/bonopo/master_v2`)

Declaration of honour

Hereby I declare that the work was done independently and only using the specified resources.

Freiburg, April 2, 2019 Signature

Bibliography

Arnell, N. W. (1999). The effect of climate change on hydrological regimes in Europe: a continental perspective. *Global environmental change 9*(1), 5–23.

Bachmair, S., I. Kohn, and K. Stahl (2015). Exploring the link between drought indicators and impacts. *Natural Hazards and Earth System Sciences 15*(6), 1381–1397.

Bachmair, S., M. Tanguy, J. Hannaford, and K. Stahl (2018). How well do meteorological indicators represent agricultural and forest drought across Europe? *Environmental Research Letters 13*(3), 034042.

Barker, L. J., J. Hannaford, A. Chiverton, and C. Svensson (2016). From meteorological to hydrological drought using standardised indicators. *Hydrology and Earth System Sciences 20*(6), 2483–2505.

Beguería, S. and S. M. Vicente-Serrano (2017). SPEI: Calculation of the Standardised Precipitation-Evapotranspiration Index. R package version 1.7.

Beguería, S., S. M. Vicente-Serrano, F. Reig, and B. Latorre (2014). Standardized precipitation evapotranspiration index (SPEI) revisited: parameter fitting, evapotranspiration models, tools, datasets and drought monitoring. *International Journal of Climatology 34*(10), 3001–3023.

Beyene, B., A. Van Loon, H. Van Lanen, and P. Torfs (2014). Investigation of variable threshold level approaches for hydrological drought identification. *Hydrology and Earth System Sciences 11*(11), 12765–12797.

BGR (2016). Bundesanstalt für Geowissenschaften und Rohstoffe: Hydrogeologische Übersichtskarte von Deutschland 1:200.000, Oberer Grundwasserleiter (HÜK200 OGWL). *Digitaler Datenbestand 3*.

Birsan, M.-V., P. Molnar, P. Burlando, and M. Pfaundler (2005). Streamflow trends in switzerland. *Journal of Hydrology 314*(1-4), 312–329.

Bloomfield, J. P., D. J. Allen, and K. J. Griffiths (2009). Examining geological controls on baseflow index using regression analysis: An illustration from the Thames Basin, UK. *Journal of Hydrology 373*(1-2), 164–176.

Bloomfield, J. P. and B. P. Marchant (2013). Analysis of groundwater drought building on the standardised precipitation index approach. *Hydrology and Earth System Sciences 17*(12), 4769–4787.

Briffa, K. R., G. van der Schrier, and P. D. Jones (2009). Wet and dry summers in Europe since 1750: Evidence of increasing drought. *International Journal of Climatology 29*(13), 1894–1905.

Brunetti, M., M. Maugeri, T. Nanni, I. Auer, R. Böhm, and W. Schöner (2006). Precipitation variability and changes in the greater alpine region over the 1800–2003 period. *Journal of Geophysical Research 111*(D11).

Burke, E. J., S. J. Brown, and N. Christidis (2006). Modeling the Recent Evolution of Global Drought and Projections for the Twenty-First Century with the Hadley Centre Climate Model. *Journal of Hydrometeorology 7*(5), 1113–1125.

Burn, D. H. and M. A. Elnur (2002). Detection of hydrologic trends and variability. *Journal of hydrology 255*(1-4), 107–122.

Carsten F. Dorman (2012). Parametrische Statistik: Verteilungen, maximum likelihood und GLM in R.

Ceballos, A., J. Martinez-Fernandez, and M. A. Luengo-Ugidos (2004). Analysis of rainfall trends and dry periods on a pluviometric gradient representative of Mediterranean climate in the Duero Basin, Spain. *Journal of Arid Environments 58*(2), 215–233.

Christensen, J. H. and O. B. Christensen (2003). Climate modelling: Severe summertime flooding in Europe. *Nature 421*(6925), 805.

Clausen, B. and C. P. Pearson (1995). Regional frequency analysis of annual maximum streamflow drought. *Journal of Hydrology 173*(1-4), 111–130.

Coch, A. and L. Mediero (2016). Trends in low flows in Spain in the period 1949–2009. *Hydrological Sciences Journal 61*(3), 568–584.

Dai, A. (2011). Drought under global warming: a review. *Wiley Interdisciplinary Reviews: Climate Change 2*(1), 45–65.

Douglas, E. M., R. M. Vogel, and C. N. Kroll (2000). Trends in floods and low flows in the United States: impact of spatial correlation. *Journal of Hydrology 240*(1-2), 90–105.

Drápela, K., I. Drápelová, et al. (2011). Application of mann-kendall test and the sen's slope estimates for trend detection in deposition data from bílý kříž (beskydy mts., the czech republic) 1997-2010. *Beskydy 4*(2), 133–146.

Epule, T. E., C. Peng, and L. Lepage (2015). Environmental refugees in sub-saharan africa: a review of perspectives on the trends, causes, challenges and way forward. *GeoJournal 80*(1), 79–92.

European Environment Agency (2016). Snow cover.

Fleig, A. K., L. M. Tallaksen, H. Hisdal, and S. Demuth (2006). A global evaluation of streamflow drought characteristics. *Hydrology and Earth System Sciences 10*(4), 535–552.

Forzieri, G., L. Feyen, R. Rojas, M. Flörke, F. Wimmer, and A. Bianchi (2013). Ensemble projections of future streamflow droughts in europe. *Hydrology and Earth System Sciences 18*, 85–108.

Ganguli, P. and A. R. Ganguly (2016). Space-time trends in U.S. meteorological droughts. *Journal of Hydrology: Regional Studies 8*, 235–259.

Gilbert, R. O. (1987). *Statistical methods for environmental pollution monitoring*. John Wiley & Sons.

Gobiet, A., S. Kotlarski, M. Beniston, G. Heinrich, J. Rajczak, and M. Stoffel (2014). 21st century climate change in the European Alps—A review. *Science of The Total Environment 493*, 1138 – 1151.

Gosling, S. N., J. Zaherpour, N. J. Mount, F. F. Hattermann, R. Dankers, B. Arheimer, L. Breuer, J. Ding, I. Haddeland, R. Kumar, D. Kundu, J. Liu, A. van Griensven, T. I. E. Veldkamp, T. Vetter, X. Wang, and X. Zhang (2016, nov). A comparison of changes in river runoff from multiple global and catchment-scale hydrological models under global warming scenarios of 1°C, 2°C and 3°C. *Climatic Change 141*(3), 577–595.

Groisman, P. Y., R. W. Knight, and T. R. Karl (2001). Heavy precipitation and high streamflow in the contiguous United States: Trends in the twentieth century. *Bulletin of the American Meteorological Society 82*(2), 219–246.

Guha-Sapir, D., D. Hargitt, and P. Hoyois (2004). Thirty years of natural disasters 1974-2003: The numbers. *Presses univ. de Louvain*.

Gustard, A. and S. Demuth (2009). Manual on low-flow estimation and prediction. *WMO-No. 1029*.

Haied, N., A. Foufou, S. Chaab, M. Azlaoui, S. Khadri, K. Benzahia, and I. Benzahia (2017). Drought assessment and monitoring using meteorological indices in a semi-arid region. *Energy Procedia 119*, 518–529.

Hanel, M., O. Rakovec, Y. Markonis, P. Máca, L. Samaniego, J. Kyselỳ, and R. Kumar (2018). Revisiting the recent European droughts from a long-term perspective. *Scientific reports 8*(1), 9499.

Hasselmann, K. (1993). Optimal fingerprints for the detection of time-dependent climate change. *Journal of Climate 6*(10), 1957–1971.

Hasselmann, K. (1998). Conventional and bayesian approach to climate-change detection and attribution. *Quarterly Journal of the Royal Meteorological Society 124*(552), 2541–2565.

Haylock, M., N. Hofstra, A. K. Tank, E. Klok, P. Jones, and M. New (2008). A european daily high-resolution gridded data set of surface temperature and precipitation for 1950–2006. *Journal of Geophysical Research: Atmospheres 113*(D20).

Heinrich, B. and C. Leibundgut (2000). WaBoA-Wasser-und Bodenatlas Baden-Württemberg.

Hellwig, J. and K. Stahl (2018). An assessment of trends and potential future changes in groundwater-baseflow drought based on catchment response times. *Hydrology and Earth System Sciences Discussions*, 1–26.

Hellwig, J., K. Stahl, M. Ziese, and A. Becker (2018). The impact of the resolution of meteorological data sets on catchment-scale precipitation and drought studies. *International Journal of Climatology 38*(7), 3069–3081.

Helsinki Commission (2013). Climate change in the Baltic Sea Area HELCOM thematic assessment in 2013. *Baltic Sea Environment Proceedings No. 137*.

Hoerling, M., S. Schubert, K. Mo, A. Aghakouchak, H. Berbery, J. Dong, et al. (2013). An interpretation of the origins of the 2012 central great plains drought. *Assessment Report from the NOAA Drought Task Force Narrative Team*.

Huang, S., P. Li, Q. Huang, G. Leng, B. Hou, and L. Ma (2017). The propagation from meteorological to hydrological drought and its potential influence factors. *Journal of Hydrology 547*, 184–195.

Hundecha, Y. and A. Bárdossy (2005). Trends in daily precipitation and temperature extremes across western Germany in the second half of the 20th century. *International Journal of Climatology*.

KLIWA (2005). Langzeitverhalten des Gebietsniederschlags in Baden-Württemberg und Bayern. *KLIWA - Berichte 7*.

Koffler, D., T. Gauster, and G. Laaha (2016). *lfstat: Calculation of Low Flow Statistics for Daily Stream Flow Data*. R package version 0.9.4.

Kohnová, S. and J. Szolgay (2000). Regional estimation of design flood discharges for river restoration in mountainous basis of Northern Slovakia. In *Flood issues in contemporary water management*, pp. 41–47. Springer.

Kulkarni, A. and H. von Storch (1995). Monte carlo experiments on the effect of serial correlation on the mann-kendall test of trend. *Meteorologische Zeitschrift 4*(2), 82–85.

Laaha, G. and G. Blöschl (2006). Seasonality indices for regionalizing low flows. *Hydrological Processes 20*(18), 3851–3878.

Livezey, R. A. and W. Y. Chen (1983). Statistical field significance and its determination by Monte Carlo techniques. *Monthly Weather Review 111*(1), 46–59.

Machiwal, D. and M. K. Jha (2012). *Hydrologic time series analysis: theory and practice*. Springer Science & Business Media.

Marx, A., R. Kumar, S. Thober, O. Rakovec, N. Wanders, M. Zink, E. F. Wood, M. Pan, J. Sheffield, and L. Samaniego (2018). Climate change alters low flows in Europe under global warming of 1.5, 2, and 3°C. *Hydrology and Earth System Sciences 22*(2), 1017–1032.

Matalas, N. C. and W. Langbein (1962). Information content of the mean. *Journal of Geophysical Research 67*(9), 3441–3448.

Mavromatis, T. and D. Stathis (2011). Response of the water balance in Greece to temperature and precipitation trends. *Theoretical and Applied Climatology 104*(1-2), 13–24.

McKee, T. B., N. J. Doesken, J. Kleist, et al. (1993). The relationship of drought frequency and duration to time scales. In *Proceedings of the 8th Conference on Applied Climatology*, Volume 17, pp. 179–183. American Meteorological Society Boston, MA.

Mäder, C., S. Richter, and H. Lehmann (2013). Globale Erwärmung im letzten Jahrzehnt? *Hintergrundpapier: Umweltbundesamt*.

Menzel, A., T. H. Sparks, N. Estrella, E. Koch, A. Aasa, R. Ahas, K. Alm-Kübler, P. Bissolli, O. Braslavská, A. Briede, et al. (2006). European phenological response to climate change matches the warming pattern. *Global change biology 12*(10), 1969–1976.

Millard, S. P. (2013). EnvStats: An R Package for Environmental Statistics.

Musselman, K. N., M. P. Clark, C. Liu, K. Ikeda, and R. Rasmussen (2017). Slower snowmelt in a warmer world. *Nature Climate Change 7*(3), 214.

Palmer, W. C. (1965). Meteorological Drought. *Research Paper* (No. 45), 58.

Parry, S., C. Prudhomme, R. L. Wilby, and P. J. Wood (2016). Drought termination. *Progress in Physical Geography 40*(6), 743–767.

Patakamuri, S. K. (2018). modifiedmk: Modified Mann Kendall Trend Tests. R package version 1.1.0.

R Core Team (2017). *R: A Language and Environment for Statistical Computing*. Vienna, Austria: R Foundation for Statistical Computing.

Radziejewski, M. and Z. W. Kundzewicz (2004). Detectability of changes in hydrological records/possibilité de détecter les changements dans les chroniques hydrologiques. *Hydrological Sciences Journal 49*(1), 39–51.

Rebetez, M., H. Mayer, O. Dupont, D. Schindler, K. Gartner, J. P. Kropp, and A. Menzel (2006). Heat and drought 2003 in Europe: a climate synthesis. *Annals of Forest Science 63*(6), 569–577.

Renard, B., M. Lang, P. Bois, A. Dupeyrat, O. Mestre, H. Niel, E. Sauquet, C. Prudhomme, S. Parey, E. Paquet, L. Neppel, and J. Gailhard (2008). Regional methods for trend detection: Assessing field significance and regional consistency. *Water Resources Research 44*(8), 289.

Samaniego, L., R. Kumar, and M. Zink (2013). Implications of parameter uncertainty on soil moisture drought analysis in Germany. *Journal of Hydrometeorology 14*(1), 47–68.

Schönwiese, C.-D. and J. Rapp (2013). *Climate trend atlas of Europe based on observations 1891–1990*. Springer Science & Business Media.

Sheffield, J., E. F. Wood, and M. L. Roderick (2012). Little change in global drought over the past 60 years. *Nature 491*(7424), 435–438.

Shukla, S. and A. W. Wood (2008). Use of a standardized runoff index for characterizing hydrologic drought. *Geophysical Research Letters 35*(2), 1100.

Spinoni, J., G. Naumann, and J. V. Vogt (2017). Pan-European seasonal trends and recent changes of drought frequency and severity. *Global and Planetary Change 148*, 113–130.

Spinoni, J., G. Naumann, J. V. Vogt, and P. Barbosa (2015). The biggest drought events in Europe from 1950 to 2012. *Journal of Hydrology: Regional Studies 3*, 509–524.

Stagge, J. H., L. M. Tallaksen, L. Gudmundsson, A. F. Van Loon, and K. Stahl (2015). Candidate distributions for climatological drought indices (SPI and SPEI). *International Journal of Climatology 35*(13), 4027–4040.

Stahl, K., H. Hisdal, J. Hannaford, L. M. Tallaksen, H. A. J. van Lanen, E. Sauquet, S. Demuth, M. Fendekova, and J. Jódar (2010). Streamflow trends in Europe: evidence from a dataset of near-natural catchments. *Hydrology and Earth System Sciences 14*(12), 2367–2382.

Steinbauer, A. and H. Komischke (2016). Klimawandel in Süddeutschland Veränderungen von meteorologischen und hydrologischen Kenngrößen - Monitoringbericht 2016. *KLIWA-Berichte*.

Tallaksen, L. M., H. Hisdal, and H. A. van Lanen (2009). Space-time modelling of catchment scale drought characteristics. *Journal of Hydrology 375*(3-4), 363–372.

Thornthwaite, C. W. (1948). An approach toward a rational classification of climate. *Geographical Review* (38), 55–94.

Trenberth, K. E., A. Dai, R. M. Rasmussen, and D. B. Parsons (2003). The changing character of precipitation. *Bulletin of the American Meteorological Society 84*(9), 1205–1218.

Umweltbundesamt (2000). CORINE Land Cover 2000 - Daten zur Landbedeckung Deutschland. DVD.

Van der Schrier, G., K. Briffa, P. Jones, and T. Osborn (2006). Summer moisture variability across Europe. *Journal of Climate 19*(12), 2818–2834.

Van Lanen, H. A. (2006). Drought propagation through the hydrological cycle. *IAHS publication 308*, 122.

van Loon, A. F. and G. Laaha (2015). Hydrological drought severity explained by climate and catchment characteristics. *Journal of Hydrology 526*, 3–14.

Vicente-Serrano, S. M., S. Beguería, and J. I. López-Moreno (2010). A Multiscalar Drought Index Sensitive to Global Warming: The Standardized Precipitation Evapotranspiration Index. *Journal of Climate 23*(7), 1696–1718.

Vicente-Serrano, S. M., J. I. López-Moreno, S. Beguería, J. Lorenzo-Lacruz, C. Azorin-Molina, and E. Morán-Tejeda (2012). Accurate Computation of a Streamflow Drought Index. *Journal of Hydrologic Engineering 17*(2), 318–332.

Vicente-Serrano, S. M., G. Van der Schrier, S. Beguería, C. Azorin-Molina, and J.-I. Lopez-Moreno (2015). Contribution of precipitation and reference evapotranspiration to drought indices under different climates. *Journal of Hydrology 526*, 42–54.

Von Storch, H. (1999). *Misuses of statistical analysis in climate research*. Springer.

Wang, G. (2005). Agricultural drought in a future climate: results from 15 global climate models participating in the IPCC 4^{th} assessment. *Climate dynamics 25*(7-8), 739–753.

Wang, J., F. Chen, L. Jin, and H. Bai (2010). Characteristics of the dry/wet trend over arid central Asia over the past 100 years. *Climate Research 41*, 51–59.

Widmann, M. and C. Schär (1997). A principal component and long-term trend analysis of daily precipitation in Switzerland. *International Journal of Climatology 17*(12), 1333–1356.

Wilks, D. S. (2011). *Statistical Methods in the Atmospheric Sciences*, Volume 100. Academic Press.

WMO (2009). WMO guidlines to Drought Indicators. *Lincoln Declaration on Drought Indices*.

Yenigün, K., V. Gümüş, and H. Bulut (2008). Trends in streamflow of the Euphrates basin, Turkey. *Proceedings of the Institution of Civil Engineers-Water Management 161*(4), 189–198.

Yu, Y.-S., S. Zou, and D. Whittemore (1993). Non-parametric trend analysis of water quality data of rivers in Kansas. *Journal of Hydrology 150*(1), 61–80.

Yue, S. and C. Wang (2004). The mann-kendall test modified by effective sample size to detect trend in serially correlated hydrological series. *Water resources management 18*(3), 201–218.

Zaidman, M. D., H. G. Rees, and A. R. Young (2001). Spatio-temporal development of streamflow droughts in north- west Europe. *Hydrology and Earth System Sciences* (5), 733–751.